JOURNAL OF GEOPHYSICAL RESEARCH, VOL. 113, D15S25, doi:10.1029/2007JD009025, 2008

Validation of Aura Microwave Limb Sounder HCl measurements

L. Froidevaux,[1] Y. B. Jiang,[1] A. Lambert,[1] N. J. Livesey,[1] W. G. Read,[1] J. W. Waters,[1] R. A. Fuller,[1] T. P. Marcy,[2,3,4] P. J. Popp,[2,3] R. S. Gao,[2] D. W. Fahey,[2] K. W. Jucks,[5] R. A. Stachnik,[1] G. C. Toon,[1] L. E. Christensen,[1] C. R. Webster,[1] P. F. Bernath,[6,7] C. D. Boone,[8] K. A. Walker,[7,9] H. C. Pumphrey,[10] R. S. Harwood,[10] G. L. Manney,[1,11] M. J. Schwartz,[1] W. H. Daffer,[1] B. J. Drouin,[1] R. E. Cofield,[1] D. T. Cuddy,[1] R. F. Jarnot,[1] B. W. Knosp,[1] V. S. Perun,[1] W. V. Snyder,[1] P. C. Stek,[1] R. P. Thurstans,[1] and P. A. Wagner[1]

Received 30 May 2007; revised 25 September 2007; accepted 31 October 2007; published 16 May 2008.

[1] The Earth Observing System (EOS) Microwave Limb Sounder (MLS) aboard the Aura satellite has provided daily global HCl profiles since August 2004. We provide a characterization of the resolution, random and systematic uncertainties, and known issues for the version 2.2 MLS HCl data. The MLS sampling allows for comparisons with many (~1500 to more than 3000) closely matched profiles from the Halogen Occultation Experiment (HALOE) and Atmospheric Chemistry Experiment Fourier Transform Spectrometer (ACE-FTS). These data sets provide HCl latitudinal distributions that are, overall, very similar to those from (coincident) MLS profiles, although there are some discrepancies in the upper stratosphere between the MLS and HALOE gradients. As found in previous work, MLS and ACE HCl profiles agree very well (within ~5%, on average), but the MLS HCl abundances are generally larger (by 10–20%) than HALOE HCl. The bias versus HALOE is unlikely to arise mostly from MLS, as a similar systematic bias (of order 15%) is not observed between average MLS and balloon-borne measurements of HCl, obtained over Fort Sumner, New Mexico, in 2004 and 2005. At the largest pressure (147 hPa) for MLS HCl, a high bias (~0.2 ppbv) is apparent in analyses of low to midlatitude data versus in situ aircraft chemical ionization mass spectrometry (CIMS) HCl measurements from the Aura Validation Experiment (AVE) campaigns in 2004, 2005, and 2006; this bias is also observed in comparisons of MLS and aircraft HCl/O_3 correlations. Good agreement between MLS and CIMS HCl is obtained at 100 to 68 hPa. The recommended pressure range for MLS HCl is from 100 to 0.15 hPa.

Citation: Froidevaux, L., et al. (2008), Validation of Aura Microwave Limb Sounder HCl measurements, *J. Geophys. Res.*, *113*, D15S25, doi:10.1029/2007JD009025.

1. Introduction

[2] Measurements of stratospheric chlorine species are an essential part of the observational strategy for understanding the impact of anthropogenic emissions of chlorofluorocarbons (CFCs) on stratospheric ozone. Measurements of the main active chlorine compound, chlorine monoxide (ClO) have been performed from space since the 1991 launch of the Microwave Limb Sounder (MLS) on the Upper Atmosphere Research Satellite (UARS) [e.g., *Waters et al.*, 1996; *Froidevaux et al.*, 2000; *Santee et al.*, 2003]. Ground-based measurements of ClO have also provided relatively long term information on active chlorine [*Solomon et al.*, 2006]. Time series of the abundances for the main chlorine reservoirs have been obtained from ground-based measurements of (column) hydrogen chloride (HCl) and chlorine nitrate ($ClONO_2$) [*Rinsland et al.*, 2003; *Mahieu et*

[1]Jet Propulsion Laboratory, California Institute of Technology, Pasadena, California, USA.
[2]Earth System Research Laboratory, NOAA, Boulder, Colorado, USA.
[3]Also at Cooperative Institute for Research in Environmental Sciences, University of Colorado, Boulder, Colorado, USA.
[4]Now at Milwaukee, Wisconsin, USA.
[5]Harvard-Smithsonian Center for Astrophysics, Cambridge, Massachusetts, USA.
[6]Department of Chemistry, University of York, York, UK.
[7]Also at Department of Chemistry, University of Waterloo, Waterloo, Ontario, Canada.
[8]Department of Chemistry, University of Waterloo, Waterloo, Ontario, Canada.
[9]Department of Physics, University of Toronto, Toronto, Ontario, Canada.
[10]School of GeoSciences, University of Edinburgh, Edinburgh, UK.
[11]Also at New Mexico Institute of Mining and Technology, Socorro, New Mexico, USA.

0148-0227/08/2007JD009025$09.00

al., 2004; *Schneider et al.*, 2005]. Stratospheric HCl profiles have been measured continuously from late 1991 through November 2005 by the Halogen Occultation Experiment (HALOE), as part of the UARS mission [*Russell et al.*, 1996; *Anderson et al.*, 2000]. Early stratospheric chlorine reservoir data were provided by measurements from balloon and aircraft [e.g., *Webster et al.*, 1993, 1994], as well as from the Space Shuttle Atmospheric Trace Molecule Spectroscopy (ATMOS) observations [e.g., *Zander et al.*, 1996]. More recently, ACE on SCISAT-1 [*Bernath et al.*, 2005; *Rinsland et al.*, 2005; *Nassar et al.*, 2006] and MLS on Aura [*Waters et al.*, 2006, *Santee et al.*, 2008] have provided additional space-based global measurements of chlorine species (ClO, $ClONO_2$, HCl).

[3] The 15 July 2004 launch of the Aura satellite, with four remote sensors on board [*Schoeberl et al.*, 2006], has led to a new and extensive data set about the Earth's atmospheric composition. This includes continuous (day and night) global measurements by the MLS instrument, which detects thermal emission lines from many trace gases at millimeter to submillimeter wavelengths (see the overview description by *Waters et al.* [2006]); EOS MLS will mostly be referred to in this work as MLS, or Aura MLS. Upper stratospheric HCl data from Aura MLS have excellent sensitivity from daily repeatable coverage with sampling of 1.5° or better in latitude, and have already provided a global average consistency check on the expected rate of decline for total stratospheric chlorine [*Froidevaux et al.*, 2006b]. That work used MLS version 1.51 data from August 2004 through January 2006 and explored differences between various satellite measurements of HCl, in the context of longer-term chlorine variations; error estimates were also provided for the v1.51 HCl data. The MLS version 1.52 software algorithms have been producing the MLS "standard HCl" product since 16 February 2006, but using slightly different frequency channels (from MLS band 14). This change was put in place after anomalous electronic gain degradation was noticed in early 2006 in the original MLS band (band 13) targeting HCl, albeit with no immediate impact to the calibrated radiances. The band 13 channels have been deactivated since 16 February 2006, except for occasional days as a diagnostic. Besides the use of different continuously operating channels to retrieve HCl, there have been other changes in version 2.2 (e.g., in the retrievals of temperature and tangent pressure) that indirectly affect the HCl profiles, in comparison to v1.52 (or v1.51) data; these changes have benefited the MLS ozone retrievals [*Froidevaux et al.*, 2008]. For 15 February 2006 and preceding days, the MLS v2.2 software also produces a separate "HCl-640-B13" product (in the MLS Level 2 diagnostic files), using the band 13 radiances; this product has slightly better precision and vertical resolution in the upper stratosphere than the v2.2 HCl standard product (from MLS band 14). MLS HCl data continuity across the mid-February 2006 time period requires the use of a consistent data version (v2.2) since the Aura launch.

[4] Version 2.2 represents the 2nd public release of MLS data, and has been used for "forward processing" since March 2007; version 2.2 is in the reprocessing stage as well, with a much more limited set of days currently available than from version 1.5. We focus on version 2.2 here, since this is considered to be the most definitive version to date. We use several months of (noncontiguous) version 2.2 data covering late 2004 to early 2007, with an emphasis on special months or days of interest for validation (including balloon and aircraft campaigns). As an example, comparisons between MLS and HALOE require days prior to December 2005, with fewer than 100 d of reprocessed MLS data available, at the time of writing; we will see that this number of days is certainly sufficient to draw robust conclusions. We note that a subsequent data version, labeled 2.21, includes a minor software patch that affects the treatment of bad MLS Level 1 radiances, but with essentially no impact, in comparison to version 2.20, on the days that are reprocessed; the available version 2.20 data can therefore be used "as is," and we refer to these days (and other days using version 2.21) collectively as version 2.2, or v2.2. Earlier validation analyses using v1.5 data were performed [*Froidevaux et al.*, 2006a] for January through March 2005. Some perspective with respect to the original (v1.51) MLS data will be provided in many of the comparisons discussed here, although the overall MLS HCl results have not changed in a very significant way.

[5] A more in-depth validation analysis is provided here than in the early MLS validation results of *Froidevaux et al.* [2006a], who used MLS v1.5 data over a specific and limited time period (January–March 2005). Section 2 gives a detailed description of the MLS measurements, from (Level 1) spectral radiances and residuals to (Level 2) retrievals and characterization of uncertainties; this goes beyond the upper stratospheric HCl error analysis provided by *Froidevaux et al.* [2006b], while confirming the overall nature of those results. Section 3 provides an array of comparisons between the MLS HCl profiles and correlative HCl profiles from both "routinely acquired" satellite measurements and "campaign-related" data sets (from balloons and aircraft), geared specifically toward Aura validation. While there is some value in comparing HCl column measurements to columns obtained from an integration of the MLS HCl profiles, we focus here on higher-resolution profile comparisons and global spatial distributions; temporal changes, including variations in HCl column abundances, are not considered in this validation paper using available (and somewhat limited in temporal extent) version 2.2 MLS data.

2. MLS Measurements

[6] After a brief review of MLS and its measurements in section 2.1, we present typical Level 1 radiance spectra and residuals relevant to HCl in section 2.2. Section 2.3 summarizes the data usage and screening recommendations for the v2.2 HCl profiles, on the basis of analyses of reprocessed data available at the time of writing. Sections 2.4 and 2.5 provide a detailed description of estimated MLS HCl uncertainties, both random and systematic, which we refer to as precision and accuracy. Section 2.6 discusses the changes in HCl from v1.5 to v2.2, both in the retrieval approach and in the average abundances, as well as in the estimated precision and actual scatter in the profiles.

2.1. Overview

[7] MLS measures millimeter and submillimeter emission by scanning the Earth's atmospheric limb every 24.7 s in a direction ahead of the Aura satellite, which is in a sun-

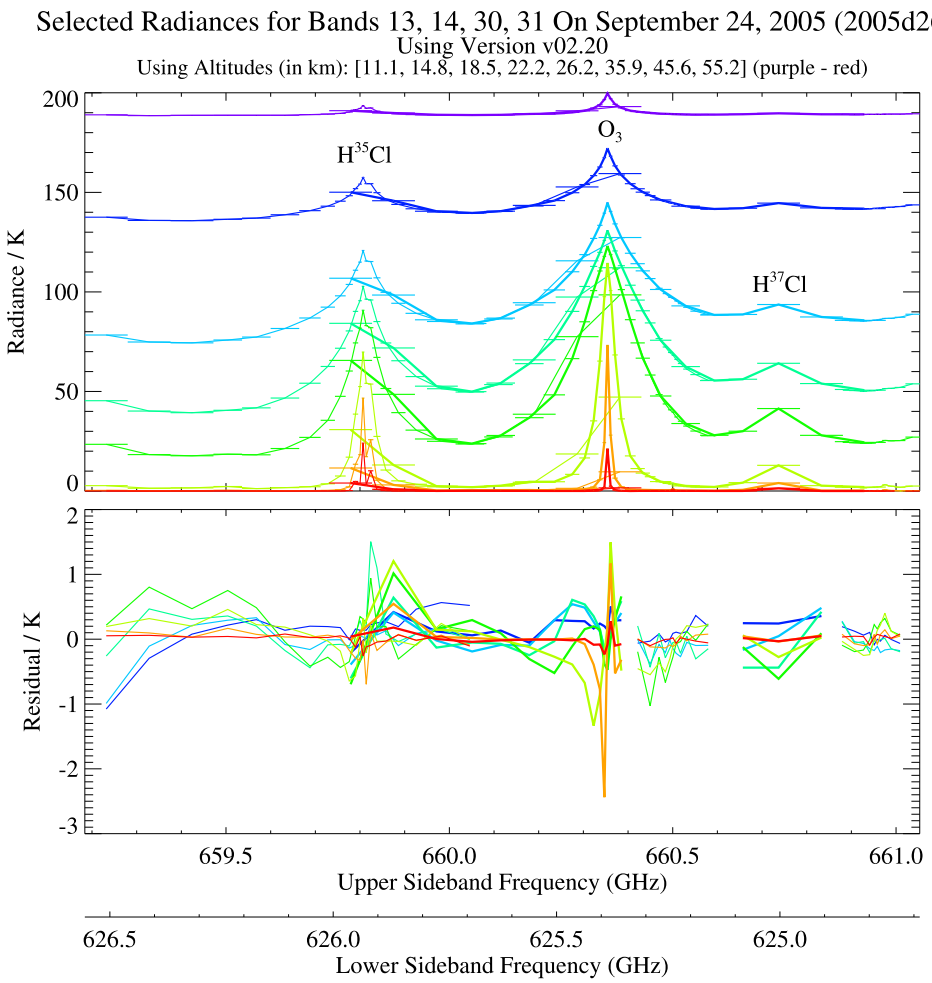

Figure 1. (top) MLS daily average radiances for 24 September 2005 for the spectral region near 630 GHz, relevant to the retrievals of HCl. These radiances are given for average tangent heights of 11 km (purple) to 55 km (red), as indicated above the plot. The *x* axes provide the frequencies in the upper and lower sidebands, which both contribute to the total radiances measured by MLS. The thick colored lines join the channels from MLS band 14 (centered on the ozone feature labeled "O_3"), with channel widths indicated by horizontal lines. This band covers the $H^{35}Cl$ emission at 626 GHz (on the left) and the weaker $H^{37}Cl$ isotope emission (on the right) and is being used for reprocessing of v2.2 data and the current v2.2 retrievals (since March 2007). MLS band 13, centered on the $H^{35}Cl$ emission, with channels joined by thin colored lines, was used for v1.5 data until 15 February 2006; the use of band 13 was discontinued because of degradation in its signal chain electronics. (bottom) Residuals (average calculated minus observed radiances) corresponding to each colored curve from Figure 1 (top). Channels that are not shown in this panel (e.g., for 11 km) are not used in the HCl retrievals.

synchronous near-polar orbit with ~1345 local equatorial crossing time (ascending node), thus providing retrievals of daytime and nighttime profiles roughly every 165 km along the suborbital track. The instrument observes five broad spectral regions between 118 GHz and 2.5 THz, covered by seven radiometers. For an overview of the MLS instrument, observational characteristics, spectral bands, main line frequencies, and target molecules, see *Waters et al.* [2006]. Vertical scans are synchronized to the Aura orbit, leading to retrieved profiles at the same latitude every orbit, with a spacing of 1.5° great circle angle along the suborbital track; the 240 limb scans per orbit provide close to 3500 profiles per day, stored in Level 2 data files, in Hierarchical Data Format (more specifically, of the HDF-EOS 5 format type). The vertical retrieval is on a pressure grid with 6 levels (pressure surfaces) per decade change in pressure in the stratosphere, and with 3 levels per decade for pressures smaller than 0.1 hPa. The MLS data from the first two public data versions are available from the NASA Goddard Spaceflight Center Distributed Active Archive Center (DAAC), specifically the Goddard Earth Sciences (GES) Data and Information Services Center (DISC), at http://disc.gsfc.nasa.gov/Aura/MLS/index.shtml. Public information about MLS and MLS data access, as well as MLS-related publications, can be found at the MLS website (http://mls.jpl.nasa.gov).

[8] The radiometric and spectral performances of the GHz radiometers are discussed by *Jarnot et al.* [2006].

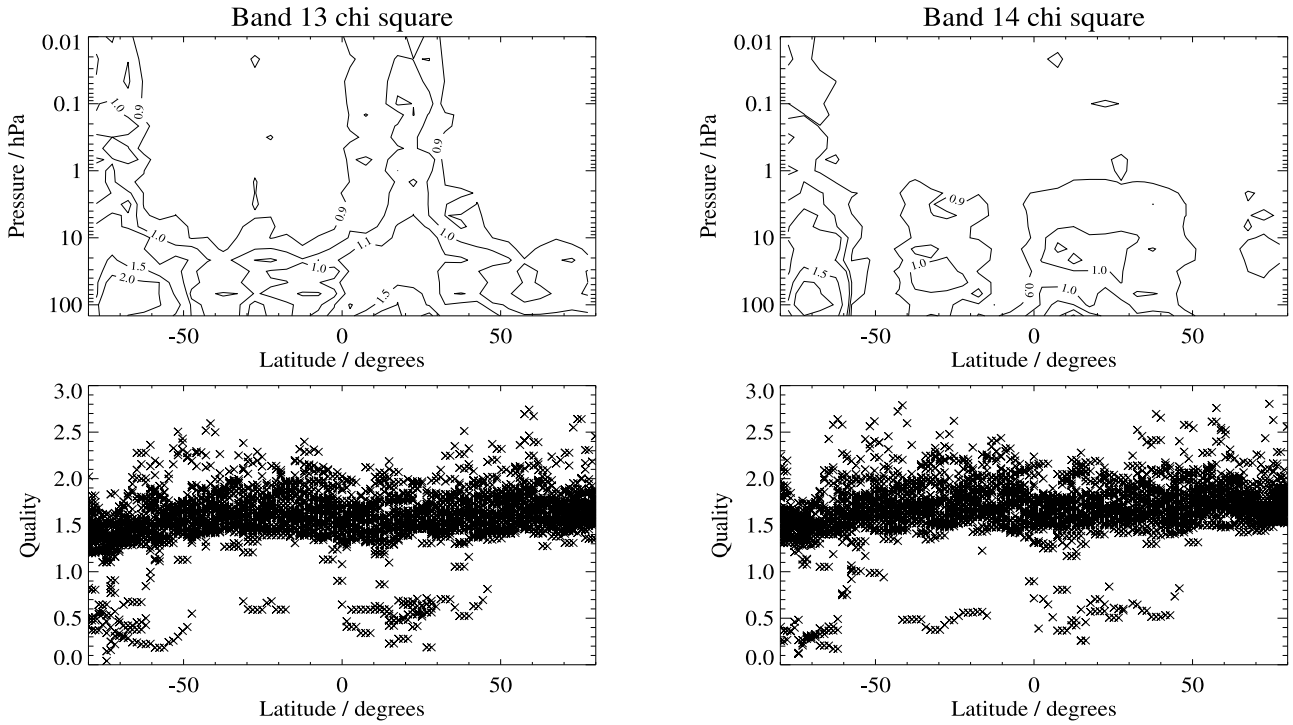

Figure 2. (top) Zonal mean chi square values (see text) representing the goodness of radiance fits versus latitude and pressure for 11 September 2005. (top left) Band 13 results and (top right) band 14 results. Results from these two bands are well correlated (see also Figure 2 (bottom)), implying that HCl retrieval quality behaves in a similar way for these two cases (v2.2 uses band 14, whereas v1.51 used band 13). (bottom) Values of the related HCl "Quality" field, which provides a single number as a measure of the radiance fits, for each of the 3494 retrieved profiles. (bottom left) Results for band 13 and (bottom right) results for band 14.

The MLS retrieval approach is given by *Livesey et al.* [2006] and the calculation specifics of the MLS radiance model (or "forward model") are described by *Read et al.* [2006] and *Schwartz et al.* [2006]; line of sight gradients are taken into account in these retrievals.

2.2. Radiance Spectra and Residuals

[9] Retrieved MLS HCl profiles come largely from HCl rotational emission lines near 625.92 GHz measured by the 640 GHz radiometer (R4), originally in band 13 (using the MLS nomenclature). This radiometer also targets nearby spectral lines (at 625.37 GHz) from ozone, using band 14 (which is not the primary band near 240 GHz used for the "standard" ozone product from MLS), as well as much less prominent features from BrO (band 31) and HO_2 (band 30). Profiles of N_2O, ClO, and HOCl are also retrieved using R4 radiances, in a spectral region from 635 to 653 GHz. Sample calculated spectra for all MLS radiometer signals are shown by *Read et al.* [2006], who also provide typical measured mean spectra and corresponding radiance precisions. Typical radiance spectra and accompanying residuals are shown in Figure 1 for the spectral region relevant to HCl. This illustrates daily averaged radiances from the ozone and $H^{35}Cl$ lines, including the weaker nearby isotopic $H^{37}Cl$ line. Figure 1 shows radiances arising from various tangent heights, from the upper troposphere (near 11 km) to the lower mesosphere (near 55 km), where the lines are much narrower. The average residuals in Figure 1 are obtained from average calculated (forward model) radiances minus measured radiances; the calculated radiances use one full day of atmospheric profiles (trace gases and temperature) retrieved by the MLS v2.2 algorithms. The same patterns for average radiances and residuals are evident if we use the same day, but a year apart (not shown here); such calculations are performed daily for all MLS bands. The typical residuals obtained from Figure 1 are of order 0.1 to

Table 1. Meaning of Bits in the "Status" Field

Bit	Value[a]	Meaning
0	1	flag: do not use this profile (see bits 8–9 for details)
1	2	flag: this profile is "suspect" (see bits 4–6 for details)
2	4	unused
3	8	unused
4	16	information: this profile may have been affected by high-altitude clouds
5	32	information: this profile may have been affected by low-altitude clouds
6	64	information: this profile did not use GEOS-5 temperature a priori data
7	128	unused
8	256	information: retrieval diverged or too few radiances available for retrieval
9	512	information: the task retrieving data for this profile crashed (typically a computer failure)

[a]"Status" field in L2GP file is total of appropriate entries in this column.

1 K; this compares to signal strengths (spectral contrast above the baseline being important here) of order 50 K, so the residuals are of order 1%. Remaining small radiance differences are expected to contribute only in a small way to errors in the retrieved product. On the basis of radiance noise of order 1 to 4 K for individual measurements from this band [see *Waters et al.*, 2006], the expected precision for daily averages (with more than 3000 spectra per day at each height) is less than 0.1K. There is therefore a small but systematic component in these residuals (typical of other days' results, not shown here), and removing or further reducing such systematics is a desired task for a future MLS retrieval version.

[10] Pressure/latitude contour plots of typical daily zonal mean "chi square" values for the MLS bands (band 13 and band 14) sensitive to HCl are shown in Figure 2 (top); these values provide an average representation of the sum of the squared radiance residuals divided by the square of the estimated radiance uncertainties for each tangent viewing location. The median values (not shown) are typically between 1 and 2, but the average values are affected by a limited number of larger values representing poorer fits and/or fewer radiances. On the day chosen here as an example, poorer fits (larger values of chi square) are observed, in particular, at high southern latitudes and at low northern latitudes (possibly in relation to horizontal gradient issues); results from bands 13 and 14 are well correlated overall. Figure 2 (bottom) also shows the latitudinal dependence of the "Quality" values for the HCl retrievals from the two bands. "Quality" gives a simple (one number per profile) measure of radiance fits based on the overall chi square value, and is directly related to the combination of (altitude-dependent) radiance chi square values for each profile. This plot shows that minima in quality (for the poorest quality profiles) occur in the latitudinal regions where the highest zonal mean values of chi square occur; again, results from bands 13 and 14 are highly correlated. As done for v1.5 data [*Livesey et al.*, 2005], we recommend (see next section) a "Quality" threshold for screening the MLS HCl profiles.

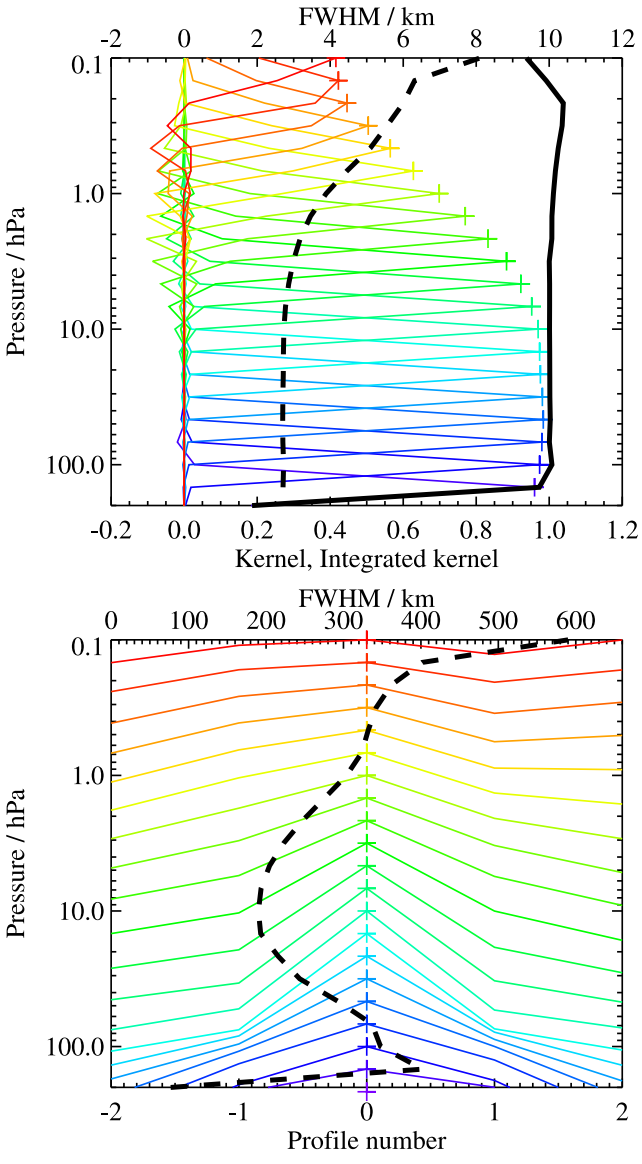

Figure 3. Representative averaging kernels (colored lines) and resolution for the v2.2 MLS standard HCl product. This example is for 35° N and results for other latitudes are very similar. (top) Colored lines show the vertical averaging kernels as a function of the MLS retrieval level, indicating the region of the atmosphere from which information is contributing to the measurements on the individual retrieval surfaces, which are denoted by the plus signs. The kernels are integrated in the horizontal dimension for 5 along-track scans. The dashed black line is the full width at half maximum (FWHM) of these averaging kernels and indicates the vertical resolution, as given in kilometers above the top axis. The solid black line shows the integrated area under each of the colored curves; a value near unity indicates that most of the information at that level was contributed by the measurements, whereas a lower value implies significant contribution from a priori information. (bottom) Colored lines show the horizontal averaging kernels (integrated in the vertical dimension) and dashed black line gives the horizontal resolution, from the FWHM of these averaging kernels (top axis, in km). The averaging kernels are scaled such that a unit change is equivalent to one decade in pressure. Profile numbers along the MLS orbit track are given on bottom axis, with negative values referring to the satellite side of the atmosphere, with respect to the tangent point profile (profile zero); profiles are spaced every 1.5° great circle angle, or about 165 km, along the orbit track.

2.3. Data Usage and Screening

[11] The following recommendations for screening the MLS HCl profiles are similar to those given for version 1.5 data [see *Livesey et al.*, 2005]. However, there are slightly different threshold values for v2.2, because of some rescaling of the relationship between radiance fits and the "Quality" flag, and there is also a new flag ("Convergence") to take into account.

2.3.1. Status Field

[12] As for v1.5 data, HCl profiles should only be used if the field named "Status" (found in the Level 2 HCl files) has an even value; this field will have an odd value if the

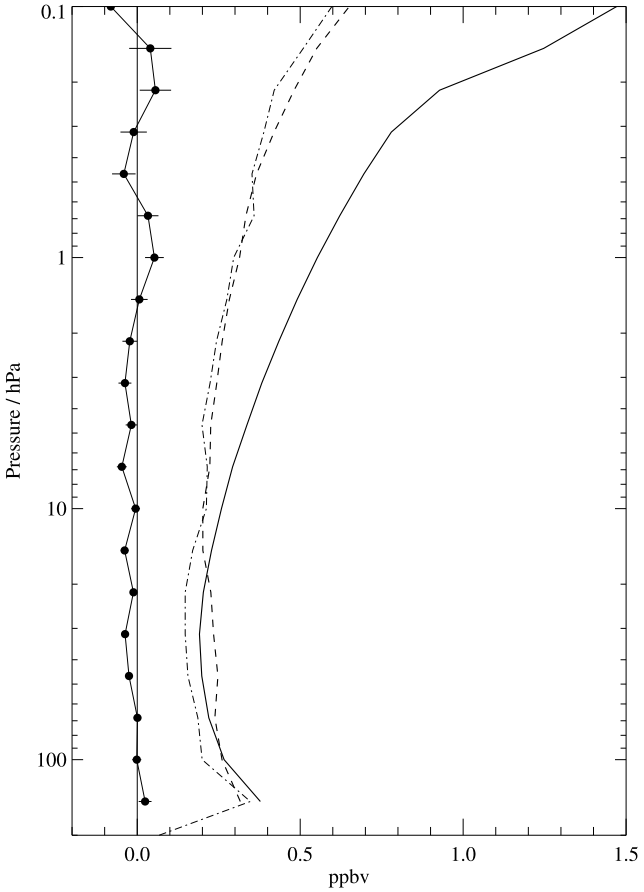

Figure 4. The estimated HCl single-profile precision as a function of pressure, for a typical day of MLS data (here, for 15 June 2005), is shown as the solid line (with no dots), based on the root mean square (rms) MLS retrieval uncertainty estimate (see text), using 741 matched profile pairs mentioned below. An empirical estimate of HCl precision (repeatability) is given by the dashed line, corresponding to the RMS scatter (divided by square root of two) about the mean differences, for all near-coincidences using both ascending and descending MLS profiles (741 matched profile pairs, using a 300 km distance matching criterion). The dash-dotted curve gives the RMS HCl variability about the mean for a narrow tropical latitude region (5°S to 5°N), where atmospheric variability is expected to be small. The mean differences between ascending and descending matched HCl profiles are given by the (connected) dots, with error bars (often smaller than the dots) indicating the precision (standard error) in these means.

retrieval diverged or not enough radiances were used, or some other anomalous instrument or retrieval behavior occurred. The retrieved profile may be considered "questionable" if "Status" is even but nonzero, in particular, if clouds may have affected some of the tangent views for a particular profile's retrieval. However, after inspecting how these profiles compare to other profiles at similar latitudes, we have found no evidence to recommend rejection of HCl profiles with such "questionable" Status values (which occur, typically, for 10–15% of the daily MLS profiles). Table 1 summarizes the various bit values that can be set and affect the value of "Status."

2.3.2. Quality Field

[13] As mentioned in the previous section, the Quality field in the Level 2 HCl files can discriminate retrieved profiles that have poor radiance fits. Specific information about which heights exhibit the worst fits are available in the MLS Level 2 diagnostic ("DGG") files, which give the height dependence of radiance chi square values. We recommend the use of HCl profiles with Quality > 1.0, in order to screen out the poorest radiance fits, typically a few percent or less, of the available daily profiles (but often ~5% in the tropics). For HCl (and the 640 GHz MLS products in general), this screening correlates well with the poorly converged sets of profiles; we recommend the use of both the Quality and Convergence field (see below) for data screening.

2.3.3. Convergence Field

[14] This new field in the L2GP files refers to the ratio of chi square value, from radiance fits for each retrieval "chunk" (typically ten profiles retrieved as a block), to the value that the retrieval would have been expected to reach. For the vast majority of HCl profiles, Convergence has values between 1 and 1.1. On occasion, sets of profiles (typically one or more "chunks") have a Convergence value larger than 1.5. These profiles usually appear to be almost noise-free and close to the a priori profile, and need to be discarded as nonconverged. The Quality field (see above) most often yields poorer quality values for these nonconverged profiles, and this typically affects a few % of the total number of (daily) profiles (including ~5% of the tropical profiles).

2.3.4. Precision Values

[15] As done before for v1.5 data, we recommend that users ignore the HCl profiles at pressures where the estimated precision values are flagged negative; at these pressures (typically only for pressures lower than 0.1 hPa), the influence of the a priori profile becomes large (estimated precision divided by a priori uncertainty becomes larger than 0.5). The pressures (in the mesosphere and troposphere) where the precision values do provide a data screening criterion generally occur at a fairly sharp transition between good and poor MLS sensitivity, although there is still some MLS sensitivity in the upper mesosphere, for example, if one uses spatially or temporally averaged abundances.

2.3.5. Vertical Range

[16] Our analyses of MLS sensitivity and precision, coupled with the characterization and validation studies described below, lead us to recommend that only MLS HCl values at pressures from 100 to 0.15 hPa be used routinely. The 147 hPa MLS retrieval level generally lies in the upper troposphere at low latitudes, but can often be in the stratosphere at high latitudes; cautious use of the high-latitude MLS HCl values at 147 hPa may be worthwhile (see details in section 3.2). The limit at 0.15 hPa is a somewhat conservative single-profile sensitivity limit, and studies of (average) HCl at higher altitudes may be performed, with caution (and preferably in consultation with the MLS team).

[17] In summary, data users should generally only use MLS HCl profiles from 100 to 0.15 hPa with (1) even value

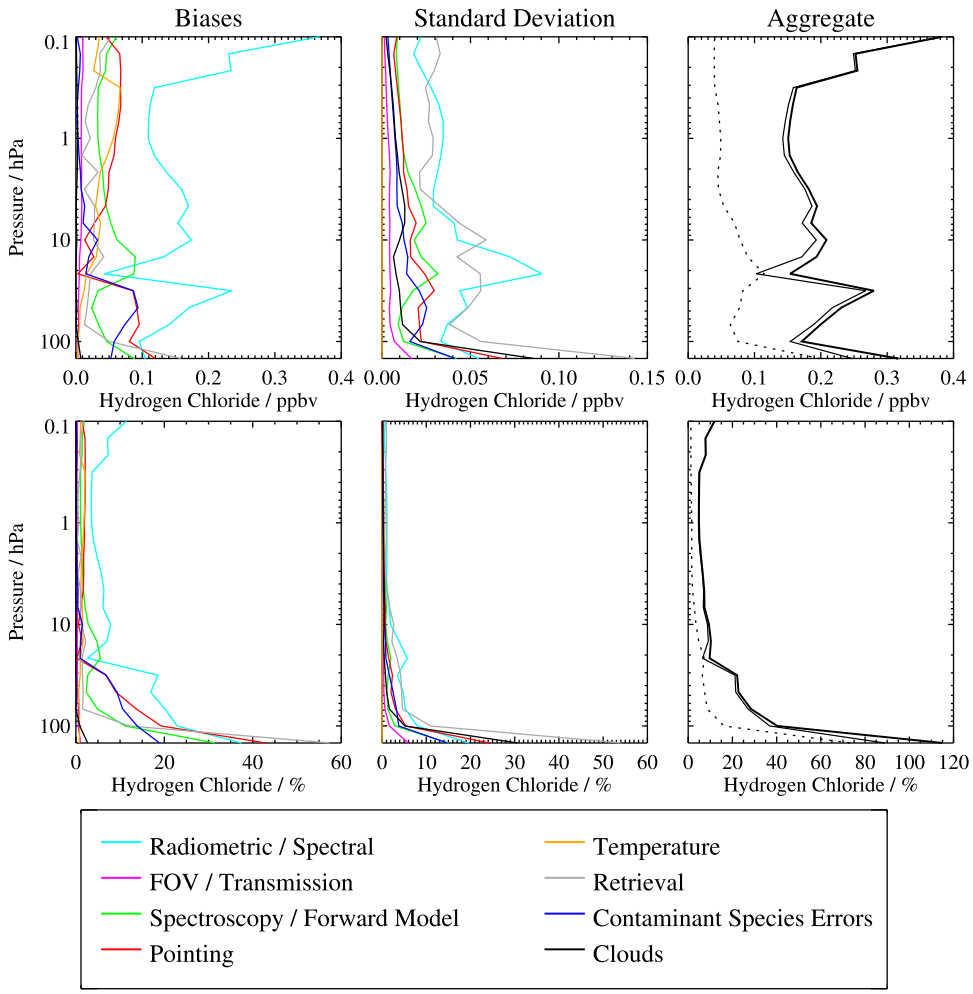

Figure 5. Estimated impact of various families of possible systematic errors on the MLS HCl measurements. (left) Possible biases and (middle) additional RMS scatter introduced by the various families of errors, with each family denoted by a different colored line. Cyan lines denote errors in MLS radiometric and spectral calibration. Magenta lines show errors associated with the MLS field of view and antenna transmission efficiency. Red lines depict errors associated with MLS pointing uncertainty. The impact of possible errors in spectroscopic databases and forward model approximations are denoted by the green line, while those associated with the retrieval numerics formulation (including sensitivity to a priori) are shown in gray. The gold lines indicate possible errors resulting from errors in the MLS temperature product, while the blue lines show the impact of similar "knock on" errors from other species (mainly from ozone and water vapor contamination). Finally, the typical impact of cloud contamination is denoted by the purple line. (right) the root sum squares (rss) of all the possible biases (thin solid line), all the additional RMS scatter (thin dotted line), and the rss of the two (thick solid line).

of Status, (2) positive precision values, (3) Quality value > 1.0, and (4) Convergence value < 1.5.

[18] These criteria should generally allow for the reliable use of more than (typically) 96–97% of the available daily MLS HCl profiles, with the precision and accuracy described later in this work being applicable.

2.4. Precision and Resolution

[19] The precision and resolution of the retrieved MLS HCl profiles limit the degree to which comparisons with other HCl profiles should agree, and the analysis and interpretation of such comparisons. The MLS antenna field of view for the 640 GHz radiometer (relevant for HCl) has a width of 1.4 km at the limb tangent point in the vertical direction, and 2.9 km in the horizontal (across-track) direction [*Waters et al.*, 2006]. The measurement resolution is also affected by the radiative transfer averaging path through the atmosphere. The resolution, both vertical and along the MLS suborbital track, can be visualized through the use of the averaging kernel matrix, as described for atmospheric retrievals by *Rodgers* [1976]. Figure 3 displays vertical and horizontal averaging kernels for a typical MLS HCl retrieval. Figure 3 also depicts (as thick dashed black lines) the corresponding vertical and horizontal resolution of the MLS HCl profiles, using the half width at full maximum

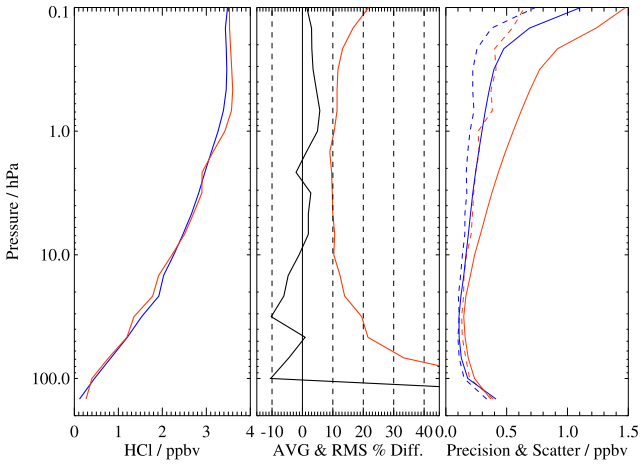

Figure 6. (left) Global mean MLS HCl abundances from versions 2.2 (red) and 1.5 (blue), based on 1 d (24 September 2004) of reprocessed MLS v2.2 data; other days lead to very similar (systematic) differences between the two data versions. (middle) Average (black) and RMS (red) HCl differences between the two data versions on this day. (right) Estimated HCl RMS precision (solid curves), as well as RMS scatter (dashed curves) about the mean in a narrow tropical latitude region (5°S to 5°N), for v2.2 data (red) and v1.5 data (blue) on this day.

of the averaging kernels as such a measure. The integrated value of the averaging kernels is generally very close to unity in the region where the influence of a priori profile information on the retrievals is negligible. For HCl, we see that this condition is satisfied from 147 to 0.1 hPa. The inferred vertical resolution is about 2.7 to 3 km from 147 to 2 hPa, with poorer resolution in the uppermost stratosphere and lower mesosphere (reaching ~6 km near 0.1–0.2 hPa). We have generated such averaging kernel plots for various latitudes and the changes for different conditions are quite small. The triangular and well-peaked nature of the averaging kernels for these limb sounding measurements is a desirable characteristic, although there are resolution limitations to keep in mind; departure from unity in the peak values of the averaging kernels in the upper stratosphere and lower mesosphere is tied to the poorer vertical resolution in this region.

[20] The precision of the HCl measurements can be arrived at from the uncertainties that are estimated by the MLS retrieval calculations, following the general *Rodgers* [1976] formulation, see *Livesey et al.* [2006]; these uncertainty estimates are provided in the MLS Level 2 files (for each profile), as the diagonal values of the error covariance matrix. Figure 4 shows typical values of this estimated precision, along with an empirical estimate from root mean square (rms) scatter about the mean for matched profile pairs from the ascending and descending portions of the orbit. Note that this scatter has been reduced by square root of two in the plot shown here, since the scatter between ascending and descending MLS profiles should be larger, by this factor, than the individual precision. The coincidence criterion chosen here, for the maximum distance separating the ascending and descending profiles, is 300 km. This scatter for ascending and descending profiles is quite similar to the RMS scatter (about the mean) within a narrow latitude bin where atmospheric variability is expected to be small (such as for 5°S to 5°N in the middle stratosphere), as shown also in Figure 4. The precision obtained empirically from the scatter in MLS profiles (dashed or dashed-dotted curves in Figure 4) is generally equal to the estimated precision for the lower stratosphere. The scatter is less than the estimated precision in the upper stratosphere and lower mesosphere by almost a factor of two, likely as a result of smoothing constraints on the MLS retrievals. The mean differences between the ascending and descending profiles (shown as dots in Figure 4) are typically very small, well under 0.1 ppbv. The MLS estimated precision for HCl does not vary much as a function of latitude (or longitude). Table 2 in section 4 summarizes the esti-mated resolution, precision, and accuracy (discussed below) for typical MLS v2.2 retrievals of HCl.

2.5. Expected Accuracy

[21] As part of the validation process, we characterize the systematic uncertainties of the retrieved profiles. Comparisons with well-characterized and accurate data can provide valuable information, but so can an assessment of known or potential error sources. Systematic errors arise from instrumental effects such as imperfect radiometric calibration or field of view characterization, as well as from errors in laboratory spectroscopic data, or retrieval formulation and implementation. This section summarizes our quantification

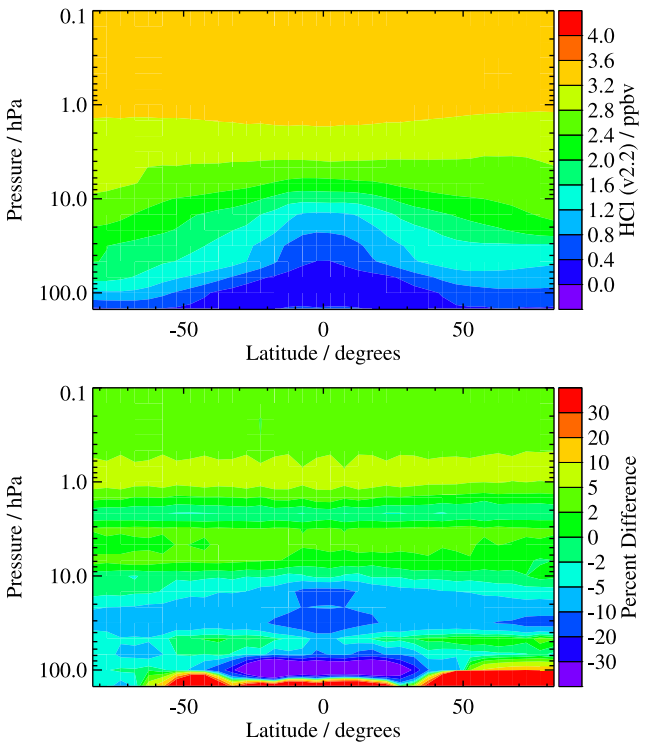

Figure 7. (top) Contour plot of the v2.2 HCl distribution versus latitude and pressure, averaged over 191 d of reprocessed MLS data. (bottom) Mean percent difference (v2.2 minus v1.5, as a percentage of v1.5 mean values) between the average MLS HCl distributions from v2.2 (above) and v1.5 (not shown, but very similar to v2.2), based on these 191 d.

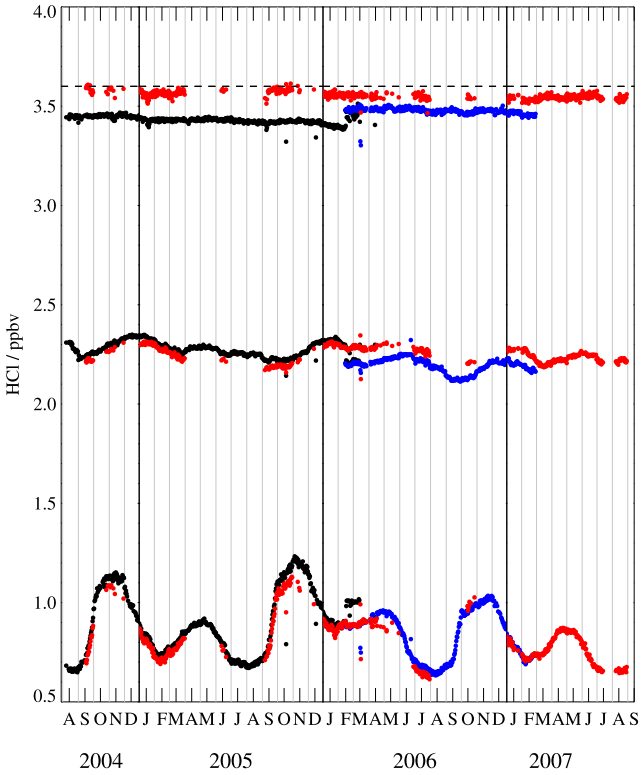

Figure 8. Time series of MLS HCl daily global means for v2.2 (one red symbol for each day available), v1.51 (black symbols), and v1.52 (blue symbols, interim data version for HCl). Top curves are for 0.5 hPa, middle curves are for 10 hPa, and bottom curves are for 68 hPa.

of these errors (uncertainties) for HCl. Details of this assessment approach are given in the Appendix material from *Read et al.* [2007]; the results provided here expand upon and supersede (but generally agree with) earlier estimates provided by *Froidevaux et al.* [2006b] for the upper stratospheric subset of the MLS HCl retrievals.

[22] For each source of systematic error, the impact on the MLS radiance measurements (or pointing, where appropriate) has been quantified and modeled. These modeled effects correspond to either 2σ estimates of uncertainty in the modeled quantity, instrument calibration uncertainty, or the sensitivity to a priori. The impact of these perturbations on retrieved MLS products has been quantified for each error source by one of two methods. In the first method, modeled errors have been applied to a whole day of simulated MLS radiances, using a three-dimensional model of the stratosphere based on a pre-Aura launch version of the SLIMCAT model [*Chipperfield*, 1999]. These perturbed radiances have then been run through the routine MLS data processing algorithms, and the systematic errors have been evaluated from the impact of the perturbation on the Level 2 products (i.e., the resulting differences from an "unperturbed" run). In addition to giving an estimate of any bias introduced by the various error sources, these "full up" studies also quantify any additional scatter (standard deviation about the mean bias) introduced in the retrievals by each error source. The difference between the retrieved product in the unperturbed run and the original "true" model atmosphere is taken as a measure of errors due to retrieval formulation and numerics. The second method for evaluating the likely impact of some remaining (typically small) systematic errors involves analytic calculations based on simplified models of the MLS measurement system [*Read et al.*, 2007]. Figure 5 provides a summary of the result of these error analyses for HCl.

[23] The results shown in Figure 5 point to possible biases of about 0.2 ppbv, with only a small amount of additional scatter in the results (the random component). Such biases translate to 5 to 10% uncertainty in the 0.1 to 20 hPa range, but increase to 20 to 40% in the lower stratosphere (30 to 100 hPa), as the HCl abundances decrease. Accuracy estimates, based on these estimated biases, are tabulated for selected pressures in the last section of this paper (see Table 2 in section 4). Results from Figure 5 and from several other more detailed analyses (not shown) of the individual components contributing to each of these families of curves [*Read et al.*, 2007] show that the major contributors to the HCl uncertainty are from radiometric and spectral calibration (cyan curves), with smaller contributions arising from possible pointing-related errors (red curves), spectroscopic errors (green curves), and in the lower stratosphere, contaminant species errors (see below). The two components that contribute the most (and roughly equally) to radiometric and spectral calibration uncertainties are gain compression effects (nonlinearities) in the MLS signal processing chains, and uncertainties in the sideband ratios (for this double sideband instrument). The spectroscopic errors are domi-

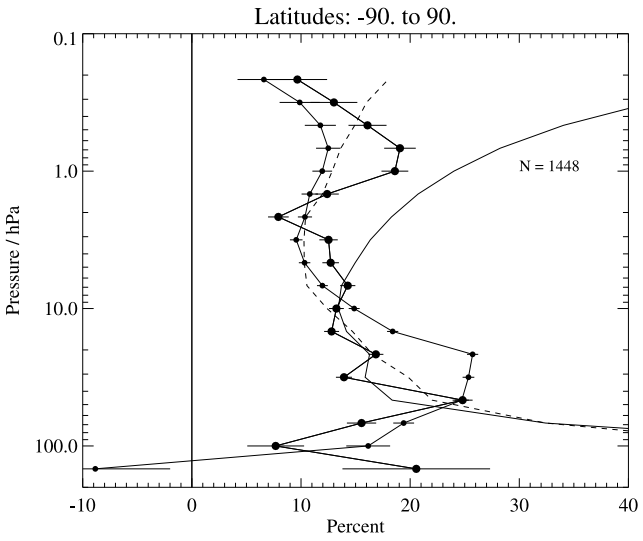

Figure 9. Global average differences between MLS and HALOE HCl profiles, based on coincident profiles obtained from over 70 d of version 2.2 MLS data in 2004 and 2005 (for 1448 matched profile pairs, as indicated by number N above); see text for coincidence criteria used. The large connected dots are for MLS v2.2 data, whereas the small dots are for v1.5 MLS data. Error bars on these dots represent twice the standard error of the mean differences. The dashed curve gives the standard deviation of the differences, and the solid curve is an estimate (see text) of the combined precision (random error) of the two measurements; both these curves are for v2.2 data.

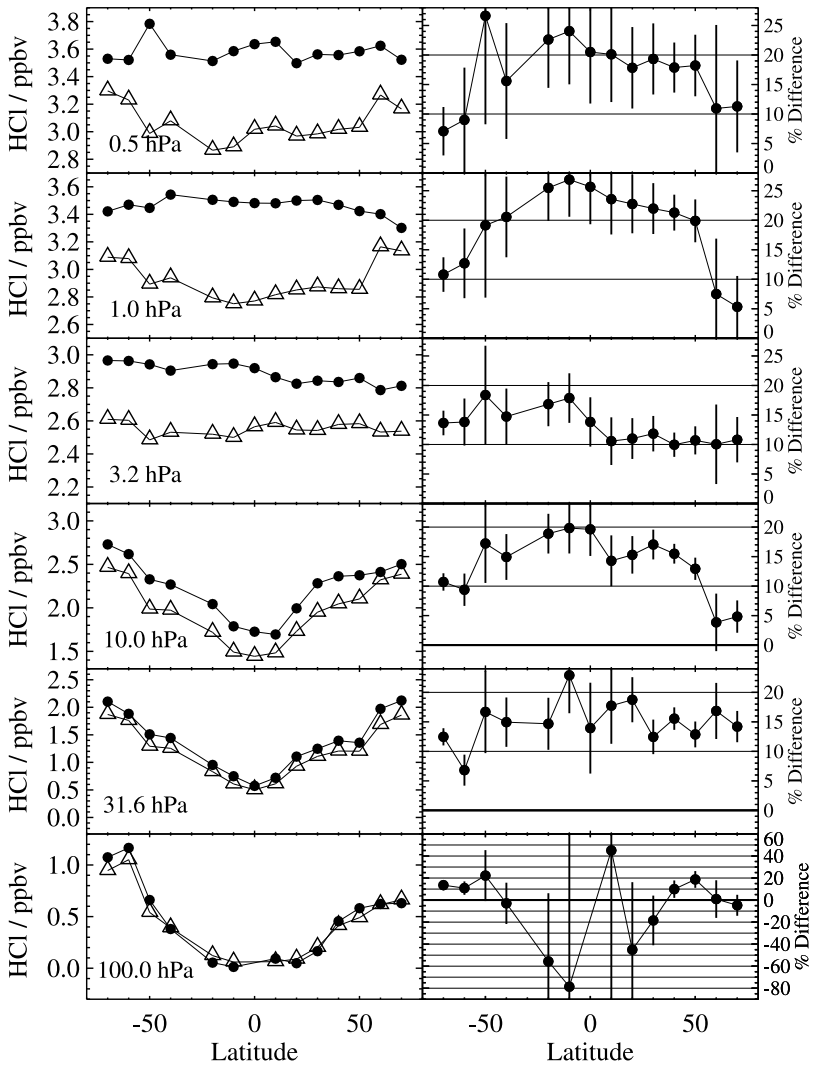

Figure 10. (left) Zonally averaged values of HCl versus latitude for coincident measurements from MLS (dots) and HALOE (triangles) at the pressures indicated in each panel. (right) HCl differences versus latitude for MLS − HALOE, as a percentage of the mean HALOE values; error bars give the (two-sigma) combined precisions in the mean differences, based on available MLS and HALOE error estimates. The data here apply to all available matched profiles from days reprocessed with MLS v2.2 data, as in Figure 9.

nated by possible errors in HCl line width (for which we use an estimated 2σ uncertainty of 5%, see *Read et al.* [2007]) and continuum emission, at the lowest stratospheric altitudes. HCl line width errors (of 5%) can lead to HCl errors of ∼5% in the lower stratosphere (and errors under 1% in the upper stratosphere), while errors in knowledge of the continuum could contribute 10–30% uncertainty at the lowest altitudes (for 100–147 hPa). At the smallest pressures shown in Figure 5 (from 0.2 to 0.1 hPa), increased uncertainties (∼5 to 10%) from possible errors in the knowledge of channel filter positions are indicated. Pointing-related errors can arise (roughly equally) from errors in the oxygen line width (assumed to be known to within 3%, see *Read et al.* [2007]), as this affects tangent pressure retrievals, and from imperfect knowledge of radiometer field of view directions, both from the absolute reference view for tangent pressure retrievals and from the relative radiometer pointing offsets. Uncertainties of more than 40% can arise from pointing-related uncertainties at the lowest retrieval altitude for HCl (147 hPa). Contaminant species errors have been assessed using estimated line width errors for the main contaminants, ozone and water vapor; the ozone line emission near the HCl line will have the largest impact (on the blue curve in Figure 5), reaching 15 to 20% near 100–150 hPa, while uncertainties from water vapor contamination may contribute significantly to (mostly random) errors (of order 15%) near 150 hPa. Finally, clouds could have some impact, mainly via poorer retrievals of tangent pressure; the proximity of clouds is determined by MLS "window channel" radiances [*Wu et al.*, 2008] and these occurrences are flagged by the MLS HCl "Status" values. We note, however, that simulated cloud-related effects (purple curves in Figure 5) do not contribute significantly to the total error for HCl. Finally, HCl errors at pressures larger than 100 hPa (see section 3.2) can be seen to arise from a combination of factors, leading to possible biases of a

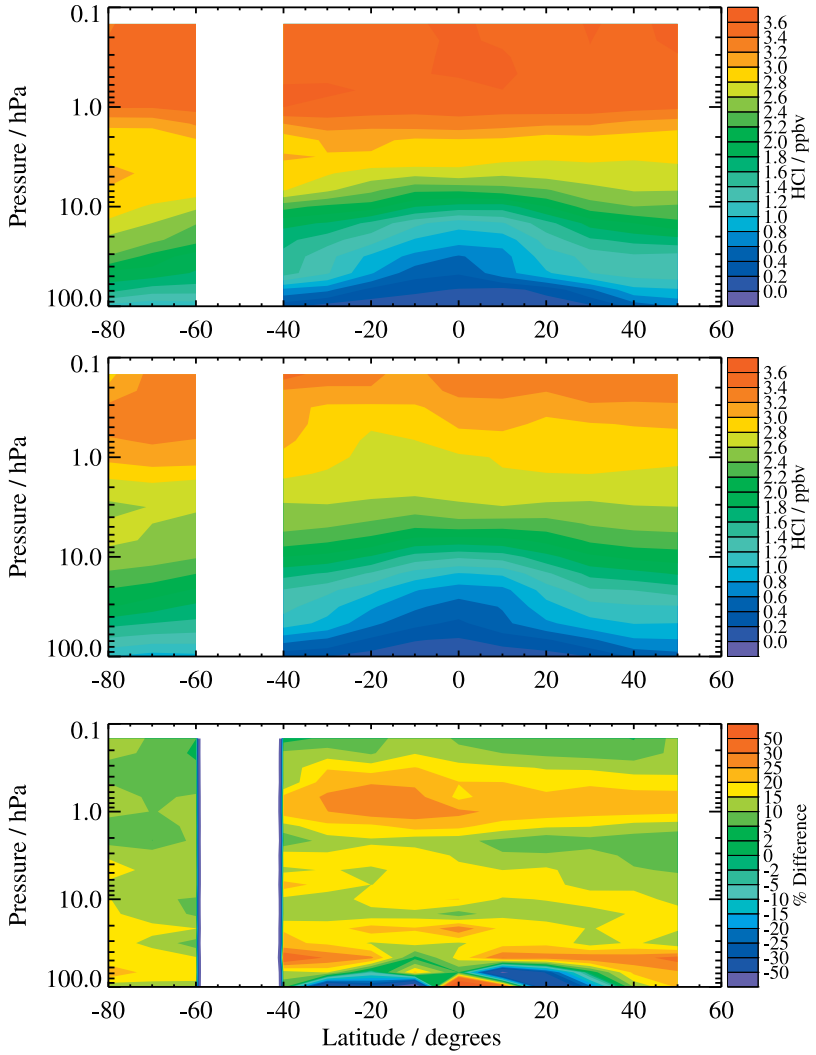

Figure 11. (top) Contour plot of zonally averaged v2.2 MLS HCl profiles versus latitude for days available from January through March 2005, including only the coincidences with available HALOE profiles. (middle) The contour plot for HALOE profiles that are matched to the MLS profiles. (bottom) Differences MLS − HALOE, as a percentage of the HALOE values.

factor of two at the lowest MLS retrieval level (147 hPa). On the basis of such error analyses for different latitude regions (not shown here), there is no strong latitudinal variation in the size (absolute or relative) of the error estimates provided in Figure 5.

2.6. Differences Between v2.2 and v1.5 Data

[24] We now discuss the changes between the v1.5 and v2.2 MLS HCl products. Besides the change (versus version 1.51) in frequency channels used now for the v2.2 retrievals (as mentioned in the introduction), v2.2 data depart somewhat from v1.51 (and v1.52) data as a result of changes to the coupled retrievals of temperature and tangent pressure, as discussed by *Schwartz et al.* [2008]. The use of slightly different bands and channels, as well as some calibration corrections for the digital autocorrelator spectrometer (DACS) channels used in these retrievals, have led to slightly lower values for the MLS temperatures, and a related shift in tangent pressure, increasing from near zero in the lower stratosphere to the equivalent of a few hundred meters near 1 hPa. Also, a finer retrieval grid is used in v2.2 retrievals for temperature (and H_2O) at pressures larger than 20 hPa, although this is not the main reason for the changes.

[25] The changes observed in MLS HCl are largely systematic in nature. Figure 6 gives a summary of the global average differences for a typical day (24 September 2004), between v2.2 and v1.51 data. The globally averaged v2.2 values are a few percent larger than v1.51 in the upper stratosphere, and 5 to 10% smaller in the lower stratosphere, with a larger percentage increase at 147 hPa, where the abundances are small. The root mean square (rms) differences are about 10% in the upper stratosphere, increasing to more than 40% in the lower stratosphere. As a result of changing from v1.5 to v2.2, the scatter in the data (from the tropical bin used for Figure 6 (right)) has increased, and the estimated precision is now a little poorer. This is because of the slightly worse sensitivity in the band 14 retrievals, as well as the use of a looser smoothing constraint in v2.2, to allow for somewhat better vertical resolution in the upper stratosphere. Figure 7 is a pressure/latitude contour plot of

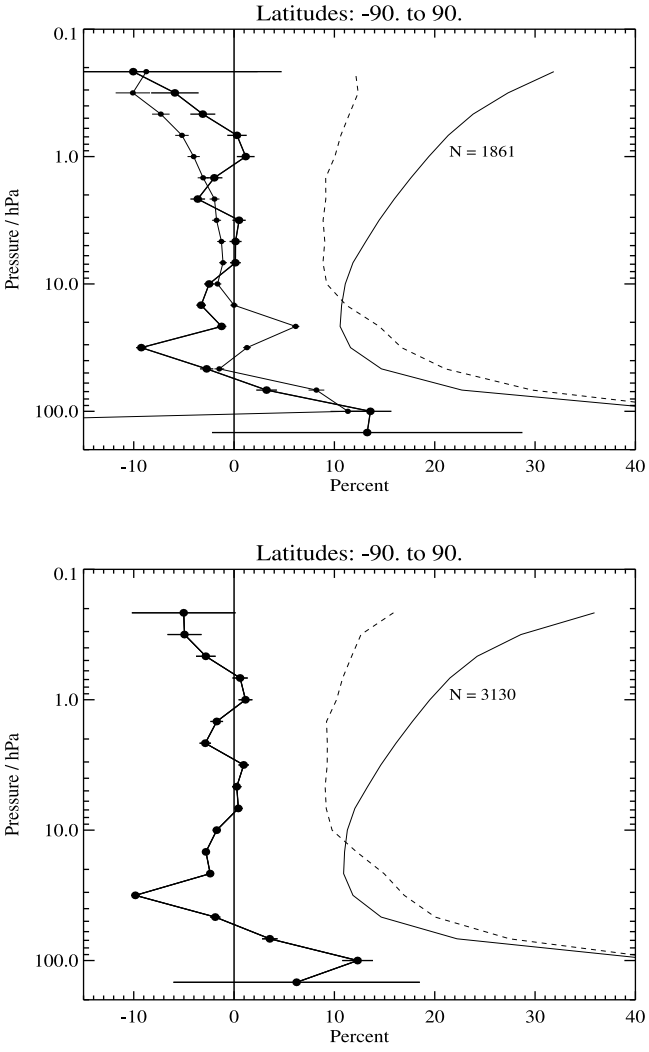

Figure 12. Similar to Figure 9 but for MLS and ACE-FTS (version 2.2) HCl differences. (top) The 1861 available matched profiles from 2004 and 2005 are compared using MLS v2.2, given as average percent difference versus ACE-FTS (large dots) as well as MLS v1.51 data (small dots). For MLS v2.2 data, the scatter between MLS and ACE-FTS is given by dashed curve, whereas the estimated combined precisions are given by the solid curve. (bottom) Same as Figure 12 (top) but for available MLS days in 2004, 2005, and 2006 data, without v1.51 data (as that consistent data version was discontinued in mid-February 2006). A total of 3130 matched profile pairs is used here for the v2.2 data (as currently available).

the average v2.2 HCl distribution and the average differences from v1.51, using available reprocessed v2.2 (and the corresponding v1.51) data. The percent changes are relatively constant as a function of latitude, except for the lowest altitudes (near 100 to 150 hPa), where the small tropical abundances lead to larger percentage variations. The average differences depicted in Figure 7 are characteristic of the zonal mean changes on any given day (as given in Figure 6) and there is a fairly small temporal variation in the differences. We do see some small but systematic oscillations in the differences between data versions; in particular, a ''notch'' of slightly lower values is observed in v2.2 data at 2.2 hPa (see Figures 6 and 7), and this is also evident in systematic differences between MLS and correlative data, as discussed later.

[26] Figure 8 shows global mean MLS HCl abundances for v2.2 and v1.5 data over available v2.2 days from August 2004 to the spring of 2007, at three selected pressures, from the lower stratosphere (68 hPa) to the uppermost stratosphere (0.5 hPa). The dashed line in this plot, for HCl at 0.5 hPa, is there to indicate that a small downward trend appears to exist in the global mean v2.2 HCl data; however, more detailed work, such as that of *Froidevaux et al.* [2006b] on upper stratospheric monthly mean HCl decreases, will be needed to provide more definitive results on longer-term variations. The use of v2.2 HCl data is required in order to avoid small, altitude-dependent, discontinuities that are currently present at the transition between the v1.51 and v1.52 data versions in mid-February 2006 (see Figure 8).

3. Comparisons With Other Data Sources

[27] We now compare MLS v2.2 HCl profiles with various data sets; v1.51 results are often included in the comparisons below, in order to illustrate (or at least summarize) the changes between the two MLS data versions.

3.1. Comparisons With Satellite Data

[28] The close to 3500 daily profiles from the currently available MLS v2.2 data provide enough comparisons for robust coincidence-type analyses versus solar occultation measurements, including detailed comparisons versus latitude.

3.1.1. MLS and HALOE Profiles

[29] Here, we use publicly available (version 19) HALOE HCl data, which are from solar occultation measurements in the infrared [*Russell et al.*, 1993], for comparison to MLS HCl. The vertical resolution of HALOE HCl is about 4 km. Following the methodology described by *Froidevaux et al.* [2006a], we compare a significant number (over a thousand in this case) of matched profiles (within 2° latitude, 8° longitude, and on the same day) from HALOE and MLS to determine average biases and related statistics between these two data sets. Our analysis here is based upon the MLS v2.2 data, as well as a larger number of matched profiles than in the earlier published v1.5 comparisons, although systematic biases of order 10% (in the middle and upper stratosphere) can be readily detected using a relatively small set (tens, not hundreds) of matched profiles. We also present latitudinal differences in more detail than in our earlier validation work.

[30] Figure 9 provides global percent differences between MLS and HALOE matched profiles from August 2004 through November 2005 (when the last HALOE measurements were taken). As expected, on the basis of the fairly small changes between MLS v1.51 and v2.2 HCl data, the previously observed biases between these two data sets have not changed dramatically. MLS HCl abundances are roughly 10 to 20% larger than the HALOE values (interpolated to the MLS pressure grid) through most of the stratosphere, and into the lower mesosphere; these average differences are statistically significant, given the error bars in Figure 9, which represent twice the standard errors

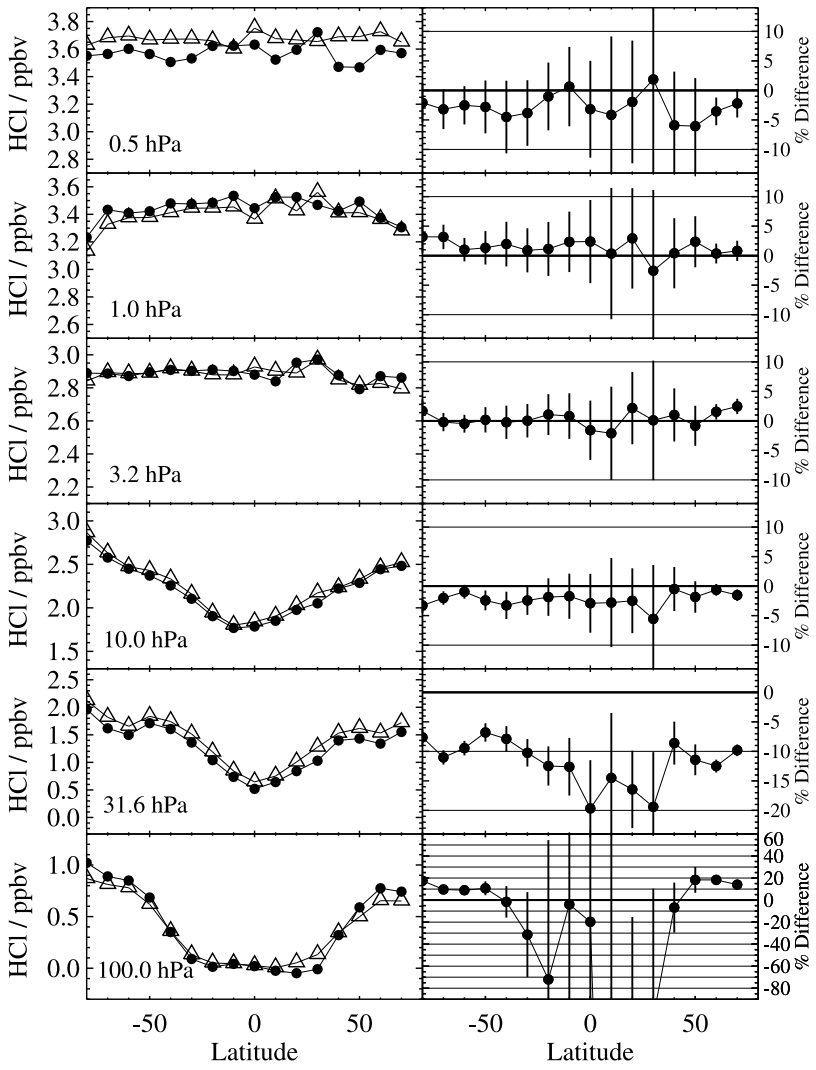

Figure 13. Similar to Figure 10 but for v2.2 MLS and ACE-FTS HCl comparisons including matched profiles from 2004, 2005, and 2006.

(precisions) in the mean differences. Although the estimated accuracies for MLS and HALOE HCl have been shown to overlap [*Froidevaux et al.*, 2006b], the HALOE HCl measurements have been consistently smaller than those from other data sets, such as balloons [*Russell et al.*, 1996], ATMOS, and ACE-FTS [*McHugh et al.*, 2005; *Froidevaux et al.*, 2006a, 2006b]. MLS v1.51 data comparisons in Figure 9 yields average results that are quite similar to those using the v2.2 data. However, some features that were mentioned in relation to Figures 6 and 7 (comparing v2.2 to v1.5 MLS data) seem to relate to the differences in Figure 9; in particular, the ''notch'' of slightly lower values (compared to adjacent pressure levels) near 2 hPa seems to be a v2.2 MLS feature, not present in the v1.5 comparisons. This may be related to a retrieval sensitivity issue in the v2.2 data (now using MLS band 14 rather than band 13), but this will require further investigations. The combined precisions of the MLS and HALOE profiles, based on the estimated uncertainties provided in the respective data files, are close to the standard deviations of the differences from all the matched profiles (see Figure 9); the somewhat smaller scatter (compared to estimated precisions) in the upper stratosphere probably arises because of a similar result in the MLS data itself, as mentioned in section 2.4.

[31] Figure 10 uses all the matched profiles that were found for the average comparisons in Figure 9, and displays the latitudinally binned averages of these profiles in Figure 10 (left), as well as their percent difference (Figure 10, right), for various pressure levels throughout the stratosphere, and up to 0.5 hPa. The latitudinal tracking between the two data sets is generally good, with relatively constant percent offsets (of order 10–20%) as a function of latitude. However, the latitudinal variations in the upper stratosphere and lower mesosphere (first and second rows in Figure 10) do not match very well and have different curvatures, especially at high latitudes. Our attempts at reducing the spatial coincidence criteria did not improve the agreement, and we do not know the reasons for these differences; however, they occur in a region of poorer precision and the differences are marginally significant, on the basis of the (two-sigma) error bars included in the difference plots. The small HCl abundances near 100 hPa at low latitudes lead to larger percent differences for this region, but the MLS and HALOE values there are most

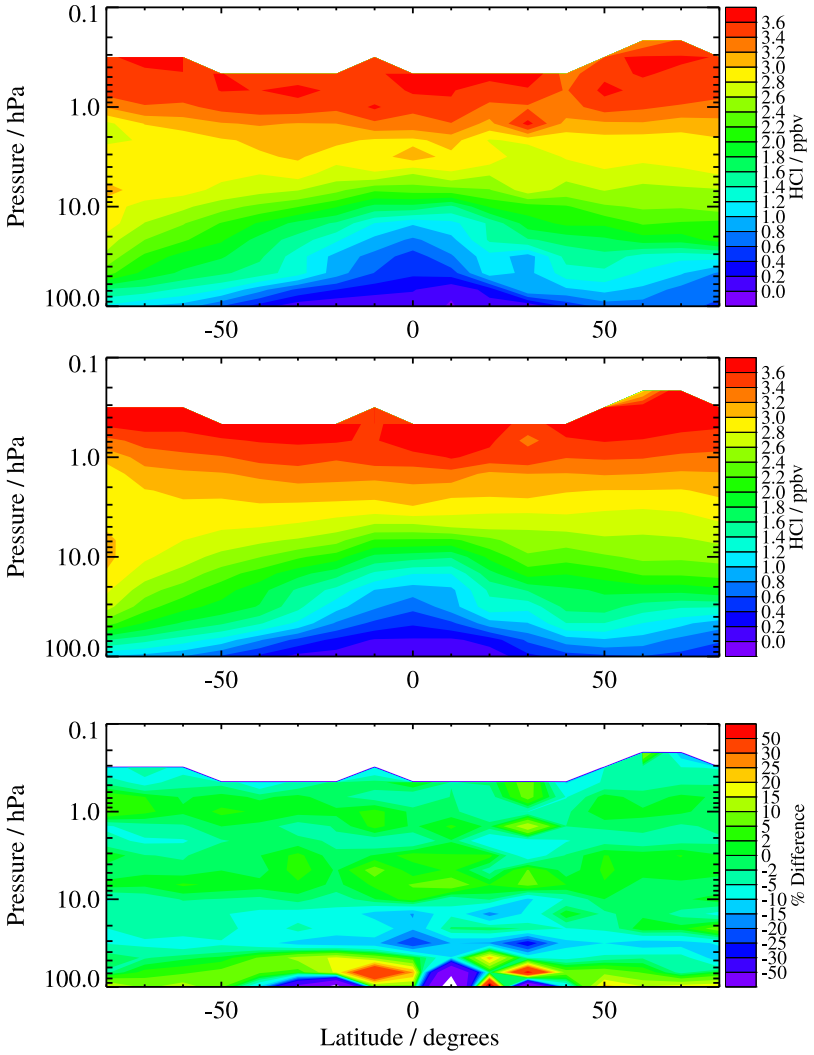

Figure 14. Same as Figure 11 but for MLS and ACE-FTS HCl comparisons.

often within ~0.1 ppbv (out of 0.1 to 0.3 ppbv). At 147 hPa, there are not enough matched comparisons for the various latitudes (mainly not enough HALOE information) to readily analyze these differences as a function of latitude for this low-altitude region. Figure 11 provides a more complete view of the altitude and latitude dependence of the MLS and HALOE HCl distributions (and their percent difference), based on matched profiles for January through March 2005. As seen in Figure 10 (which uses more available coincident profiles from 2004 through 2006), the upper stratospheric and lower mesospheric variations observed in the HALOE fields are not reproduced in the MLS fields, which tend to be flatter versus latitude, as do the ACE-FTS HCl distributions in this region (see Figure 14 below). The latitudinal gradients in the subtropics may be somewhat sharper in the MLS distribution than in the HALOE data, as mentioned by *Schoeberl et al.* [2008], although this is not (expected to be) readily apparent in this type of matched profile comparison.

3.1.2. MLS and ACE-FTS Profiles

[32] ACE-FTS [*Bernath et al.*, 2005] has provided retrievals [*Boone et al.*, 2005] since February 2004 for HCl and many other species from solar occultation observations at high resolution (0.02 cm^{-1}) in the infrared (2 to 13 μm). The ACE-FTS vertical resolution is about 3–4 km, and the retrievals are provided on a 1 km vertical grid. The analyses of the previous section are repeated for MLS HCl versus ACE-FTS HCl data, using the same coincidence criteria. The main differences being that relatively poorer sampling exists from ACE for the tropics, but a longer overlap in time and therefore more matched profiles are available (through the end of 2006) for the ACE-FTS data used here. The MLS/ACE global differences are shown in Figure 12, in a way similar to Figure 9 for the MLS and HALOE comparisons. The average agreement is excellent, with differences mostly within about 5%, certainly in the upper stratosphere, and with lower stratospheric differences centered near zero, with some 10% oscillations. Here also, the statistical case is poor for the 147 hPa pressure level. We note that the small "notch" of smaller values in the differences near 2 hPa observed in Figure 9 for MLS versus HALOE is also present in a similar way here for MLS versus ACE; this small but systematic notch exists in the MLS average profiles themselves, and this should be

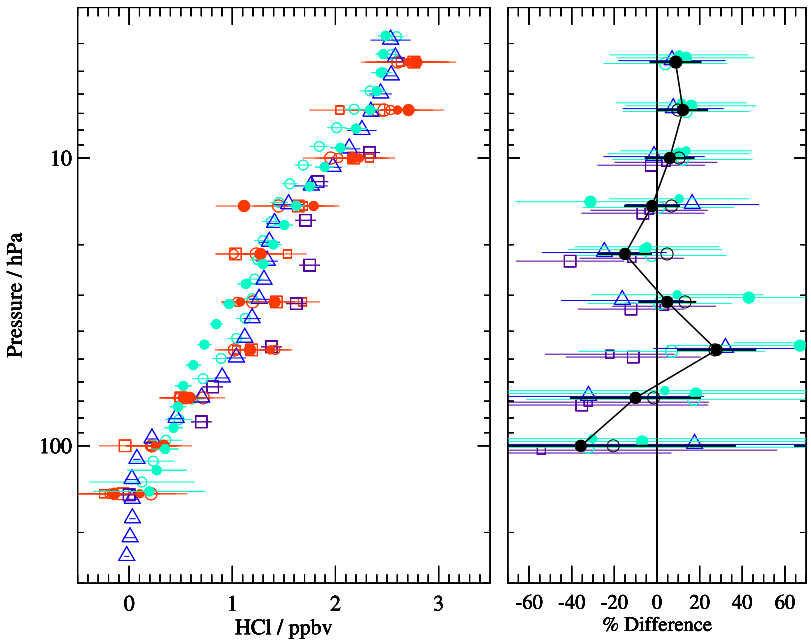

Figure 15. (left) Balloon-borne HCl measurements from Fort Sumner, in September 2004, in comparison to nearby (v2.2) MLS HCl profiles, shown as open red symbols for daytime Aura overpass and solid red circles for nighttime overpass; the two closest MLS retrievals are given (for both day and night). HCl profiles from the 23–24 September flight with FIRS-2 and MkIV measurements are shown, with FIRS-2 profiles closest in time to the daytime and nighttime MLS overpasses given by open and solid cyan circles, respectively (with error bars giving uncertainty estimates). The MkIV retrievals are shown as open blue triangles with error bars. Also shown is the comparison of MLS (daytime) HCl profiles (two closest ones) versus ALIAS-II HCl measurements from 17 September 2004, with MLS data as red squares and ALIAS data as purple squares. (right) Percent differences between MLS data from Figure 15 (left) and corresponding balloon-borne measurements (MLS closest two profiles minus balloon values, with respect to balloon values) are shown as colored symbols, for FIRS-2 day and night (open and solid cyan circles), MkIV (open blue triangles), and ALIAS-II (purple squares). The black solid circles, connected by lines, give the average percent difference from all these comparisons, using MLS v2.2 data, and the open black circles give the same but for v1.5 MLS data (individual v1.5 comparisons not shown). The error bars represent twice the expected uncertainties, for the individual points as well as for (the standard errors in) the mean differences.

investigated as part of future retrieval tests. However, it is less clear that systematic artifacts exist in the lower stratosphere, as the relative differences between MLS and HALOE do not resemble those between MLS and ACE-FTS in this region (Figure 12 versus Figure 9). Figure 12 gives the results using two time periods: one time period (Figure 12, top) uses overlap with v1.51 HCl results, covering only 2004 and 2005, and the second time period (Figure 12, bottom) covers only v2.2 MLS data, but for 2004 through 2006. The nature of the global differences is very similar for both time periods, and we note that 2004 data play a minor role in terms of the relative number of coincident profiles available here. Although this is not a rigorous test, these plots indicate that the ACE-FTS and MLS differences are fairly invariant in time, and that there are some systematic differences in these comparisons as well, even though they are significantly smaller than the MLS/HALOE differences. The comparison between estimated precisions and scatter in the differences (solid and dashed curves in Figure 12) gives results that are fairly similar to those in Figure 9, and apparently dominated by the MLS data characteristics (random noise). Figure 13 provides the latitudinal view of the matched profile distributions, using the 2004 through 2006 HCl data from MLS and ACE-FTS (with over 2200 profile pairs). Apart from the issue of low HCl in the tropics, leading to somewhat more erratic behavior in the percent differences there, there is excellent tracking as a function of latitude between these two data sets. At 100 hPa and at high latitudes, there are indications of a slightly high bias (10–20% or 0.1–0.2 ppbv), for MLS versus ACE-FTS HCl, but sorting out where the "truth" lies may prove difficult; while the respective accuracy estimates for MLS and ACE-FTS should encompass such a difference, since the MLS estimated accuracy alone is 0.15 ppbv at 100 hPa (see section 2.5 and Table 2 in section 4), this does not mean that there are no systematic biases between these two data sets. Nevertheless, the above results, as well as the MLS and ACE-FTS HCl latitudinal distributions (and differences) displayed in Figure 14 for January to March 2005, point to a very good agreement between the MLS and ACE-FTS HCl distributions.

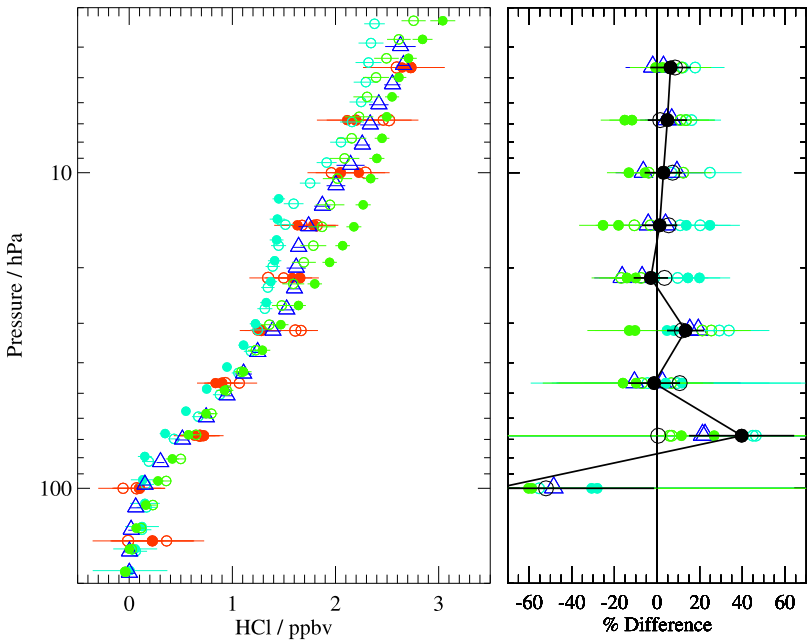

Figure 16. (left) Similar to Figure 15 but for balloon-borne Fort Sumner HCl measurements on 20 and 21 September 2005, compared to MLS (v2.2) HCl profiles, shown as open red circles for daytime, and solid red circles for nighttime overpass. FIRS-2 profiles closest in time to the daytime and nighttime MLS overpasses are shown as open and solid cyan circles, respectively; the nighttime FIRS-2 profile retrieval is limited to heights below 29 km, where most profile information exists, as the nighttime balloon float altitude dropped below this level. MkIV retrievals (sunset) are shown as open blue triangles. SLS profiles are in green (open circles for daytime and solid circles for nighttime averages). (right) Percent differences between MLS data from Figure 16 (left) and corresponding balloon-borne measurements (MLS closest two profile values minus balloon values, with respect to balloon values) are shown as colored symbols, for FIRS-2 day and night (open and solid cyan circles), for SLS day and night averages (open and solid green circles), and for MkIV data (open blue triangles). The black circles (solid for v2.2 and open for v1.5) have the same meaning (average differences) as in Figure 15.

3.2. Comparisons With Balloon Data

[33] Comparisons between MLS data and measurements from balloons launched from Fort Sumner, New Mexico, in September 2004 have been discussed by *Froidevaux et al.* [2006a]. We review the 2004 results below and include, in a similar format, HCl comparisons from the September 2005 balloon flight over Fort Sumner.

[34] In the v1.5 comparisons presented by *Froidevaux et al.* [2006a], we provided a brief description of the various balloon-borne instruments, whose measurements are used here as well. The 2005 flight included the JPL Submillimeterwave Limb Sounder-2 (SLS-2), which did not fly in 2004. This instrument obtains profiles of various trace gases, from scans of the Earth's limb thermal emission near 600 GHz; SLS-2 observes the same HCl line (near 626 GHz) as measured by Aura MLS. This new instrument includes cooled components and provides much greater sensitivity than an earlier SLS instrument. A vertical resolution of 2 to 3 km is achieved by SLS-2 and the other remote sensing balloon instruments discussed here, the JPL MkIV Fourier Transform Infrared (FTIR) spectrometer, which performs solar occultation observations in the 650 to 5650 cm^{-1} region at 0.01 cm^{-1} spectral resolution [*Toon*, 1991], and the Harvard Smithsonian Astrophysical Observatory (SAO) far-infrared spectrometer FIRS-2, measuring thermal emission at 6 to 120 μm with a spectral resolution of 0.004 cm^{-1} [*Johnson et al.*, 1995]. For the 2004 balloon comparisons, we also include (as in the earlier v1.51 results) the data from the 17 September Fort Sumner flight that provided Airborne Laser Infrared Absorption Spectrometer–II (ALIAS-II) HCl measurements, a two-channel tunable laser spectrometer using an interband cascade laser at 3.57 μm with an open-path Herriott cell (path 64 m) extending out from the gondola; absolute uncertainty in ALIAS-II HCl is about 10% or 0.1 ppbv, whichever is larger.

[35] The 2004 fall flights from Fort Sumner include the data from 23 and 24 September, with FIRS-2 and MkIV measurements of HCl, as shown in Figure 15, which provides a comparison of balloon profiles with the two closest relevant MLS profiles measured during the Aura overpass of Fort Sumner. We also show MLS HCl profiles compared to ALIAS-II in situ HCl from the 17 September 2004 balloon flight (from Fort Sumner) in Figure 15. The MLS profiles are (typically) chosen to be within 1.5° latitude and (at most) 12° longitude from the balloon measurements, which often means well within 1000 km; day and night coincidence, here, usually means that an MLS profile is within 6 h of the balloon profile(s). Figure 15 (right) gives percent differences from the (vertically interpolated) balloon data for each of the two closest relevant (day and night) MLS HCl profiles. The average percent

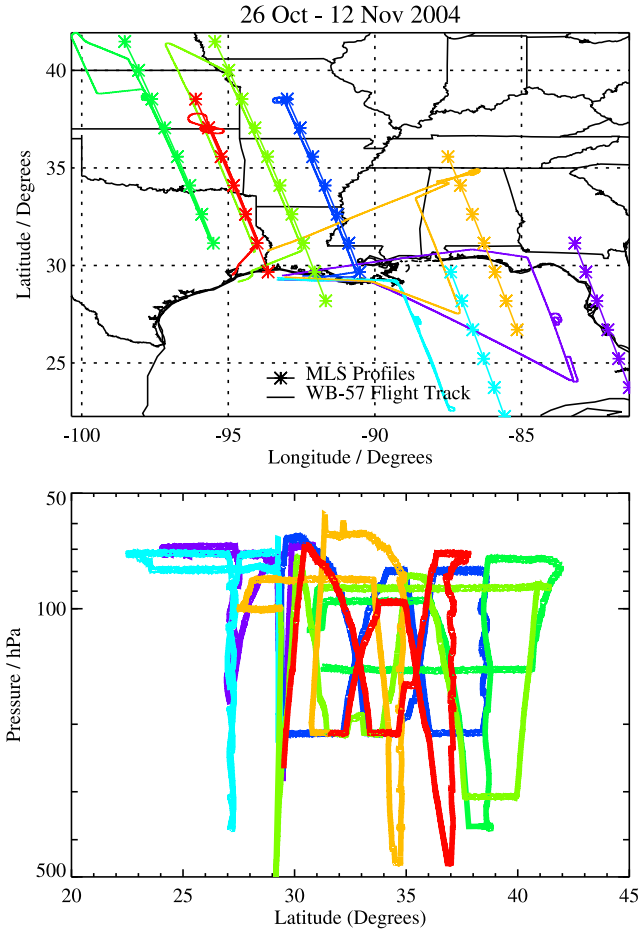

Figure 17. (top) Aircraft track locations (colored lines) during the AVE Houston 2004 campaign, compared to the location of nearby MLS daytime profile retrievals (asterisks connected by lines) for each day. The days are 26 October (purple), 29 October (blue), 31 October (cyan), 3 November (green), 5 November (light green), 9 November (gold), and 12 November (red). (bottom) The pressures sampled by the aircraft in situ HCl measurements, as a function of latitude, are shown using for each day, using the same colors as in Figure 17 (top).

differences and associated error bars (twice the standard error in the mean, using the combination of estimated uncertainties from both MLS and balloon results) from Figure 15 indicate good agreement (within the error bars) and mostly within 5 to 20%, with some oscillations about zero. The MLS HCl abundances are typically smaller than those from ALIAS-II, but larger than those from SLS-2, although absolute accuracies cannot be used to place huge significance on single flight differences, when balloon measurements themselves can also differ by more than 5–10%. Average differences between the balloon and v1.51 MLS profiles are also provided, as a reference, in Figure 15 (right), but the changes between the data versions have not significantly altered the average comparisons. A reduction in profile slope versus height is observed between about 20 and 50 hPa in the balloon data (at least for MkIV, daytime FIRS-2 and ALIAS-II profiles), and it seems that this feature (which may arise largely because of the altitude-dependent role of $ClONO_2$ in chlorine partitioning) is also present in the MLS HCl profiles.

[36] The balloon flight of 20 and 21 September 2005 lasted over 18 h at float, and sunset occultation data were obtained by the MkIV instrument. As done for the 2004 flight in Figure 15, Figure 16 displays the HCl measurements for 2005, in comparison to the two closest daytime and nighttime profiles from MLS. There were no ALIAS-II data in 2005, but the SLS-2 measurements (day and night averages) are included here, in addition to the FIRS-2 (day and night) and MkIV results. Again, we find good agreement, with MLS profiles falling in the midst of the balloon measurements. Not enough statistics are provided by large balloons since the Aura launch to enable robust conclusions regarding biases that might exceed the previously discussed MLS HCl accuracy estimates of ~5 to 15% (see Table 2 in section 4), which should be combined with the accuracy

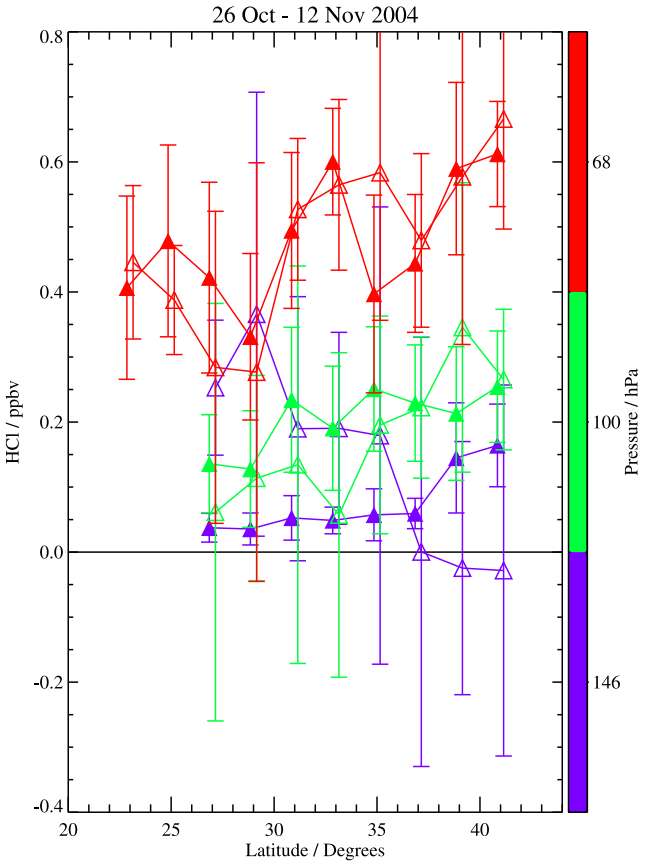

Figure 18. HCl averages versus latitude for MLS (open triangles) and CIMS (solid triangles) from a combination of all flights shown in Figure 17, using 2° latitudinal averages for both data sets. The sampled pressure ranges (color bar) represent the MLS retrievals grid points, and all the available CIMS HCl data are averaged over a range defined by the points midway between these pressure values (in log space). Error bars on each point represent the RMS variability about the averages in each latitude (and pressure) bin, over all WB-57 flights. MLS and CIMS points are offset slightly in latitude for clarity.

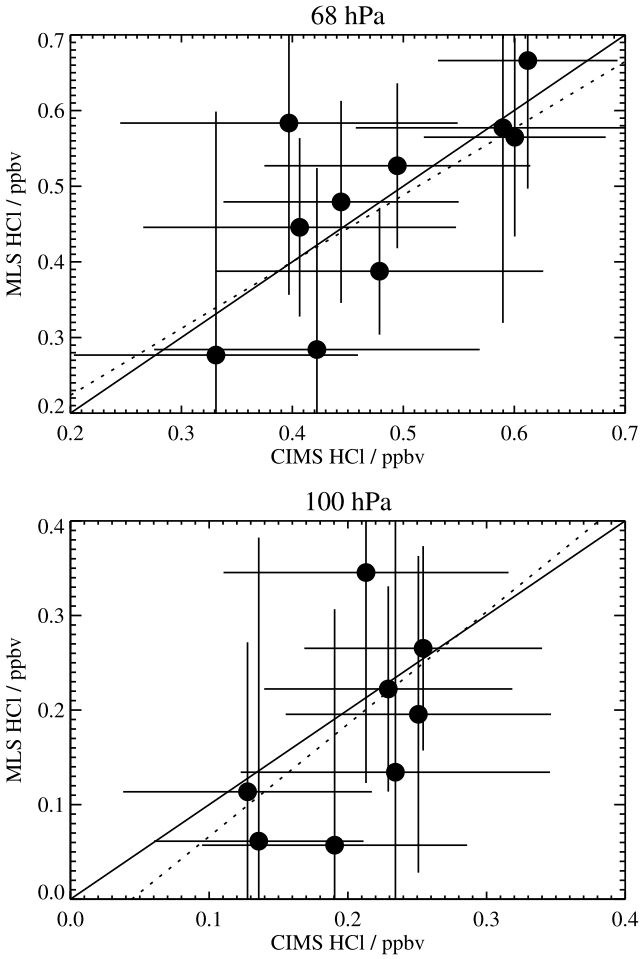

Figure 19. Scatter diagrams of MLS HCl versus CIMS HCl, using the same HCl data averages as in Figure 18, for (top) 68 hPa and (bottom) 100 hPa; the solid line gives the one-to-one correlation line, whereas the dashed line is a linear fit to the data points. The 147 hPa HCl values (see Figure 18) are not shown again here, as the correlation is quite poor, with MLS values often significantly larger than the aircraft data (see Figure 18).

estimates (typically also of order 10%) from the balloon measurements. In the context of the MLS (and ACE-FTS) high HCl biases versus HALOE data, particularly in the upper stratosphere, where satellite HCl retrievals have lower percentage uncertainties, there is only a slight indication (near 5 hPa) of a possible small MLS overestimation, in comparison to the (average) balloon results. A 15% MLS bias, the typical observed bias between MLS and HALOE HCl, seems unlikely. We note, however, that some balloon measurements start to lose sensitivity at the highest altitudes given in these plots, since some assumptions must be made about the HCl abundances (or profile shapes) at high altitude. Also, the apparent overestimate in MLS HCl in 2004 near 50 hPa is not repeated in 2005, when the largest overestimate occurs near 70 hPa. Finally, in terms of possible overestimates in MLS HCl at 147 hPa, based on the indications from the aircraft comparisons in the next section, the 2004 balloon results do not indicate a significant bias for MLS at this level; the 2005 MLS results appear to be on the high side of the balloon data at 147 hPa, but this carries marginal or no significance, given the error bars from the combination of measurements.

3.3. Comparisons With Aircraft Data

[37] A series of aircraft campaigns geared toward the validation of Aura data was put in place as a result of validation planning prior to the Aura launch [*Froidevaux and Douglass*, 2001]. Here, we compare MLS HCl profiles to available HCl data from the in situ chemical ionization mass spectrometry (CIMS) measurements obtained on a number of high-altitude WB-57 aircraft flights during these Aura Validation Experiment (AVE) campaigns, namely a fall 2004 campaign out of Houston, a summer 2005 campaign, also based in Houston, and a January/February 2006 campaign based in Costa Rica (CR-AVE 2006 campaign). The CIMS measurement technique, as described by *Marcy et al.* [2005], has a detection limit of about 0.015 ppbv (for 1s data) and accuracy of ±30% for the HCl data reported here. CIMS HCl measurements at low latitudes have previously been used to constrain the upper tropospheric HCl budget and to study stratospheric ozone inputs into the troposphere, partly through the use of HCl and ozone correlation diagrams [*Marcy et al.*, 2004].

[38] We have used MLS v2.2 HCl data for all the relevant flight days of the three campaigns mentioned above. The Houston 2004 campaign contributed the most near-coincident flights along the MLS suborbital track. We provide a number of comparison plots for this campaign, and a few key summary plots for the other two campaigns, as the main conclusions are consistent for all these campaigns. Figure 17 shows the aircraft track locations during the AVE Houston 2004 flights, along with the nearby MLS suborbital tracks and retrieved profile locations. We need to use a statistical approach for these satellite/aircraft comparisons, since the single profile precision for MLS HCl is about 0.2 to 0.4 ppbv in the 68 to 146.8 hPa retrieval range (MLS HCl is not retrieved for pressures larger than 147 hPa), and since the relevant HCl abundances measured by CIMS are typically significantly below 0.8 ppbv. The requirement for aircraft flight tracks really close to the satellite suborbital track is not overly critical here, because of the statistical approach that is needed, although close proximity of aircraft and satellite tracks should minimize potential error sources caused by lack of spatial coincidence. The temporal overlap for these comparisons is governed by the several hours needed by the WB-57 to cover the region of interest, since the satellite overpass occurs in a very short time (about two minutes). We use the continuous aircraft measurements of pressure (from NOAA) to readily interpolate the CIMS HCl time series to the appropriate pressures. Figure 17 (bottom) shows the pressures (typically between about 300 and 70 hPa) covered by the various AVE 2004 flights. We have averaged all the CIMS and MLS HCl measurements in 2° latitude bins. These averaged measurements are compared in Figure 18, using the MLS retrieval midpoints as boundaries for averaging all the available aircraft data, to better compare to MLS "points," which also represent an average over roughly this pressure range; we note that the MLS vertical resolution in this pressure range is essentially the same as the separation between the retrieval grid points. Figure 18 shows that there is fairly good tracking by MLS

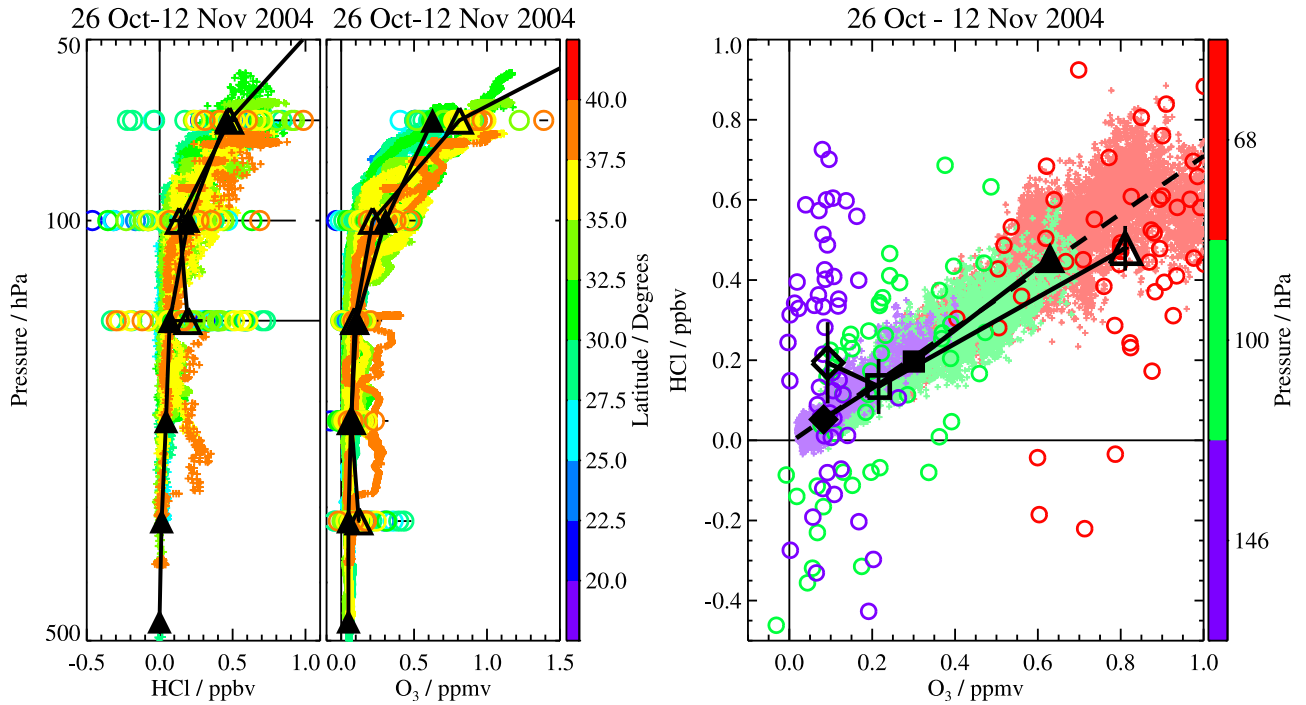

Figure 20. (left) The aggregate of all AVE Houston 2004 CIMS HCl measurements, from the flights shown in Figure 17, are shown (as a function of pressure) as small colored symbols (plus signs) along with the MLS retrieved HCl profiles (see locations in Figure 17), given by the open colored symbols. The different colors represent different latitudinal bins (see color bar at right) sampled during this campaign. For a statistically more relevant picture, averages of MLS HCl are shown as open triangles, error bars representing twice the standard errors in the means (calculated from the estimated precisions in MLS profiles), along with CIMS HCl averages (solid triangles) over the MLS-relevant pressure ranges (see Figure 18): 68, 100, and 147 hPa for the MLS retrieval levels, as well as pressures of 215, 316, and 464 hPa for additional aircraft averages (MLS a priori data exist at these levels, but no MLS retrievals are performed). A typical value of precision for MLS is given by the horizontal error bar for the maximum MLS HCl at each pressure. (middle) Same as Figure 20 (left) but for MLS and aircraft ozone measurements. (right) Scatterplot of HCl versus O_3 for all aircraft data (colored points) and all MLS profiles (open circles), color-coded by pressure (see color bar at right). The MLS and aircraft averages, given by open and solid symbols, respectively, for 68 hPa (large triangles), 100 hPa (large squares), and 147 hPa (large diamonds), are connected by thick black lines; error bars for MLS averages give twice the standard errors in the means (ozone errors are smaller than the symbols). The dashed black line is a linear fit through all the aircraft data.

of the aircraft measurements of HCl latitudinal averages and gradients for 68 and 100 hPa, within the error bars (which represent the 1σ variability within each bin). However, the 146.8 (147) hPa values from MLS are often larger than the aircraft values, and the MLS variability at this level is too large for a very conclusive comparison, based on one campaign. The correlation between MLS and CIMS HCl data (using the same averaged data as in Figure 18) is displayed in Figure 19 as a scatterplot. Again, fairly good correlation is observed between the two data sets for 68 and 100 hPa, and the fitted slopes are close to unity (within the resulting errors). The chi square values giving goodness of fit information for 68 and 100 hPa are equal to 1.3 and 0.8, respectively, and the linear correlation coefficients are equal to 0.7 and 0.6; the associated probabilities for a null hypothesis of no correlation are equal to 7 and 12%. In Figure 20, we show all available MLS and CIMS HCl measurements as a function of pressure, color-coded by latitude, and include a similar plot for the in situ measurements of ozone and the MLS ozone profiles (Figure 20, middle). The in situ ozone data were obtained from the onboard NOAA ozone instrument with a combined accuracy and precision of ±5% [*Proffitt and McLaughlin*, 1983]. The MLS ozone measurements have been shown to compare well with various data sets [*Froidevaux et al.*, 2008; *Jiang et al.*, 2007], certainly down to pressures of 147 hPa (the lowest retrieval level for HCl), including these AVE WB-57 aircraft ozone measurements [*Livesey et al.*, 2008]. Indeed, Figure 20 shows better agreement between the aircraft and MLS ozone data than for HCl, at 147 hPa; the larger average MLS ozone value at 68 hPa is probably a result of the weighting of higher altitude values in this region of rapidly increasing ozone, as the aircraft average is derived mostly from pressures larger than 70 hPa. Figure 20 (right) provides a correlation diagram between HCl and ozone measurements for all the CIMS and MLS data from

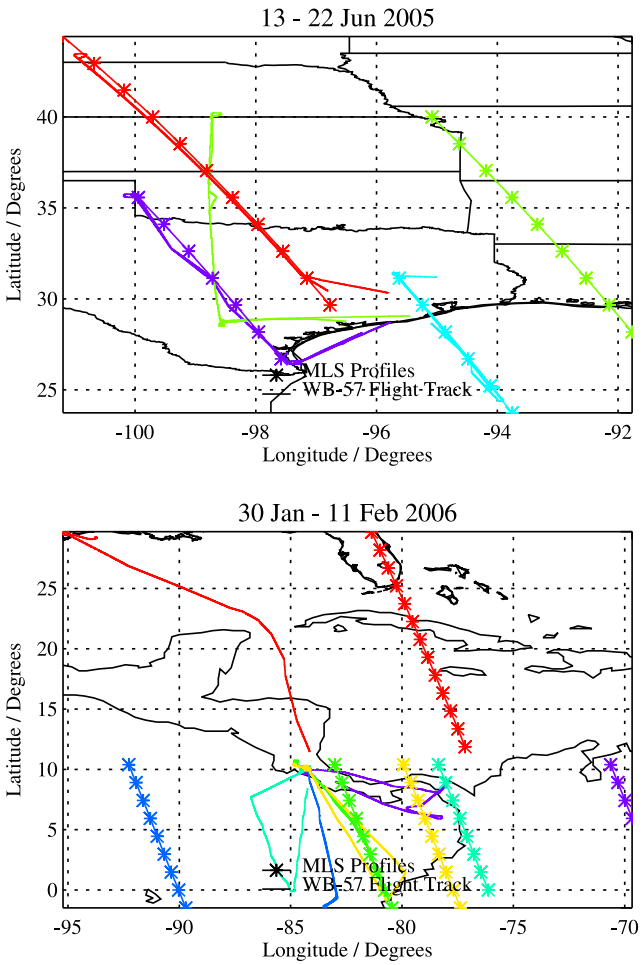

Figure 21. Same as Figure 17 but for the AVE campaigns of (top) Houston 2005 and (bottom) Costa Rica 2006 for the date ranges indicated in plot titles. The dates for each WB-57 aircraft flight are as follows: for Figure 21 (top), 13 June (purple), 15 June (cyan), 17 June (light green), and 22 June (red), and for Figure 21 (bottom), 30 January (purple), 1 February (blue), 2 February (cyan), 7 February (green), 9 February (gold), and 11 February (red).

AVE 2004. This gives a measure of the correspondence between these two atmospheric tracers, and should help reduce noncoincidence and sampling issues, even for measurements from aircraft and satellite platforms that are quite different in their intrinsic sampling characteristics. Earlier CIMS results found a linear correlation between HCl and O_3, extending from the lower stratosphere into the upper troposphere [*Marcy et al.*, 2004], as displayed here as well. The aircraft averages (solid symbols) at the three pressures are connected by a solid line, which matches well with the dashed line (linear fit through all aircraft data). The agreement between CIMS and MLS correlations is fairly good, although a few low values appear to drive the 68 hPa MLS HCl somewhat lower than the majority of aircraft data at 68 hPa. The main discrepancy that appears from these plots is the high bias in average MLS HCl at 147 hPa; note that the error bars on the MLS averages represent twice the standard error, as obtained from the estimated MLS HCl precisions.

[39] Figures 21 and 22 are a brief summary of similar comparisons for the other two campaigns, AVE 2005, and Costa Rica AVE (CR-AVE) in early 2006. Figure 21 (similar to Figure 17) displays the relevant MLS and aircraft tracks from both campaigns. Figure 22 gives the HCl profiles and the HCl versus ozone correlation plots for these two campaigns. The dynamic range of values (for both HCl and ozone) is smaller over the tropics (Costa Rica) than over Houston, as exhibited in both the MLS and aircraft data sets. We find that the HCl/O_3 correlations in the aircraft and MLS data sets at 68 and 100 hPa compare well for both of these campaigns. At 147 hPa, however, as seen in the AVE 2004 campaign, there is a high MLS HCl bias and a departure from the linear HCl/O_3 correlation observed in the higher-altitude MLS data; this also contradicts the linear relationship obtained by CIMS into the upper troposphere [see also *Marcy et al.*, 2004]. We saw in section 2.5 that errors of order 0.2 ppbv can be expected as a result of a combination of error sources (especially near 150 hPa) that could affect the MLS HCl retrievals; such an impact can become significant (more than a factor of two) where (or when) the typical HCl abundances are smaller than 0.1–0.2 ppbv; such low HCl abundances were indeed observed by CIMS, especially for pressures larger than 100 hPa in the tropics, during the CR-AVE campaign flights. This discrepancy in MLS/CIMS comparisons at the lowermost MLS retrieval level will motivate future MLS efforts for improving the satellite HCl retrievals at 147 hPa, if some of the error sources discussed in section 2 can be better characterized and taken into account.

4. Summary and Conclusions

[40] The MLS HCl version 2.2 data validation results presented here update and expand upon the v1.51 comparisons presented by *Froidevaux et al.* [2006a] and the error analyses for upper stratospheric HCl from *Froidevaux et al.* [2006b]. MLS data users should apply the data screening criteria discussed here (section 2.3) for MLS version 2.2 HCl, as there have been some changes from the screening for version 1.5. The average changes between v2.2 and v1.5 MLS HCl abundances are generally small, of order a few percent in the upper stratosphere to (occasionally) 10 percent or more in the lower stratosphere. These changes have occurred as a result of the use of frequency channels from MLS band 14 (rather than band 13), following the (early 2006) degradation and discontinuation of band 13 retrievals, as well as (indirectly) from small changes in temperature and tangent pressure results arising from the v2.2 algorithms [*Schwartz et al.*, 2008]. There are small but systematic differences between the two MLS data versions that will require further investigation. In particular, a small (few percent) negative notch that occurs at 2 hPa was not present in v1.5 MLS HCl profiles; this artifact is also observed in average comparisons versus HALOE and ACE-FTS. A continuous HCl time series from MLS requires the use of v2.2 (band 14) data, as there are small discontinuities across the "step" from v1.51 to v1.52 that occurred right after the band 13 shutdown (early on 16 February 2006). Table 2 gives a summary of the estimated resolution, precision, and

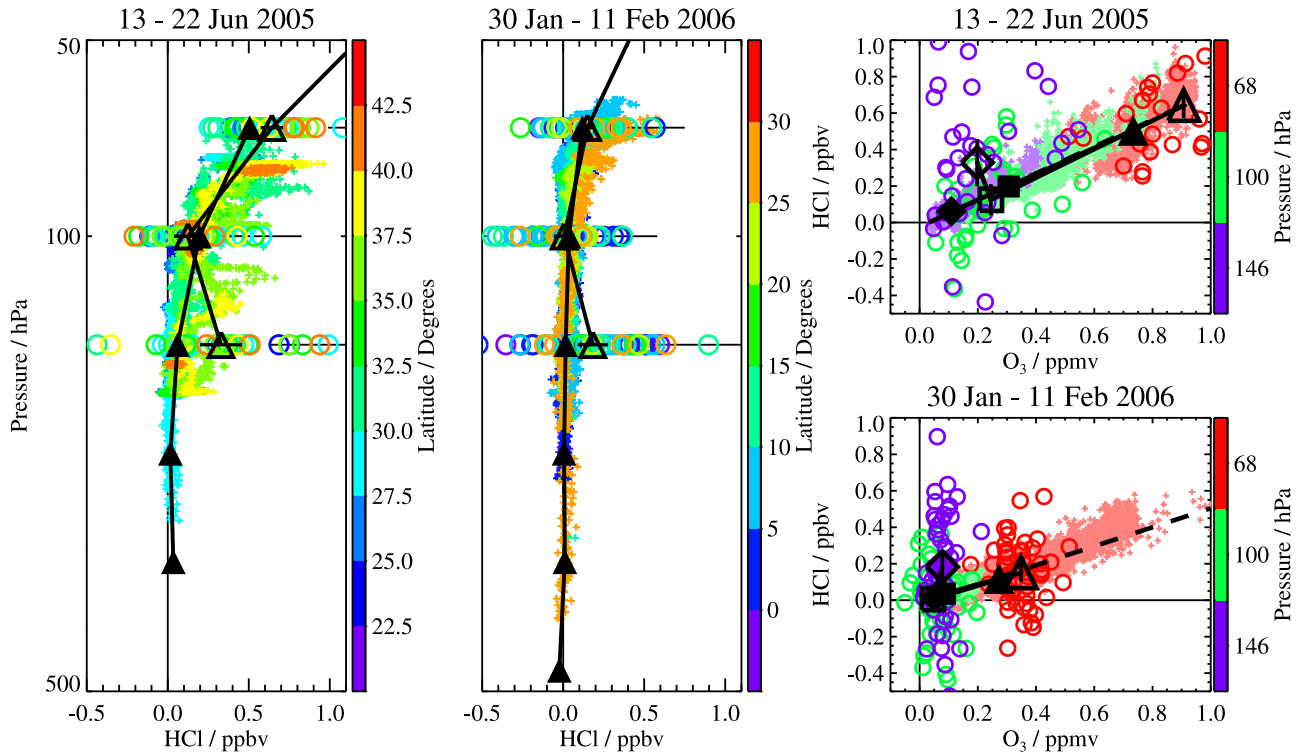

Figure 22. MLS and aircraft HCl data versus pressure (color-coded by latitude), as shown in Figure 20 (left), but here for the AVE campaigns of (left) Houston 2005 and (middle) Costa Rica 2006. (right) Scatterplots of HCl versus ozone for MLS and CIMS measurements, as shown in Figure 20 (right), but here for the (top) Houston 2005 and (bottom) Costa Rica 2006 results.

accuracy of MLS v2.2 HCl, based on the results and (rounded off) error analyses discussed in detail in this paper.

[41] The latitudinal distributions of HCl obtained using satellite profiles (from both HALOE and ACE-FTS) that coincide with available v2.2 MLS HCl retrievals from August 2004 through December 2006 show overall good agreement with the MLS latitudinal variations. However, some discrepancies between the MLS and HALOE gradients in the upper stratosphere and lower mesosphere are currently not explained. There are some systematic differences (as noted in our earlier work) in the case of (version 2.2) MLS versus (version 19) HALOE HCl, with MLS HCl abundances typically larger than those from HALOE by 10–20%; these differences are (somewhat marginally) within the accuracy estimates from both data sets [see *Froidevaux et al.*, 2006b]. As found in earlier comparisons [*Froidevaux et al.*, 2006a] coincident (v2.2) MLS and (v2.2) ACE-FTS profiles (with more than 2200 matched pairs in the current comparisons) show agreement, on average, to within 5% for most of the stratosphere. These results agree, overall, with the recent comparisons (for January 2005) provided in equivalent latitude/potential temperature coordinates by *Manney et al.* [2007], who use MLS v2.2 data. Agreement also exists between the MLS/HALOE comparisons of HCl discussed here and the analyses by *Considine et al.* [2008], who use a model initialized with MLS data to compare "forward mapped" HCl fields versus HALOE HCl measurements. *Lary and Aulov* [2008] have recently performed noncoincident analyses using probability density functions (PDFs) from MLS (v1.5) HCl and HCl measurements from HALOE and ACE-FTS; these analyses are in broad agreement with the results (biases between satellite data sets) obtained here and by *Froidevaux et al.* [2006a].

[42] Updated comparisons have been provided for HCl results of the balloon campaign from Fort Sumner, NM, in the fall of 2004. The 2005 balloon results from Fort Sumner have added consistent information, namely good agreement (mostly better than 10%) between the average balloon and MLS HCl profiles obtained during these campaigns. While it would be difficult to identify (or argue against) a 5% bias between MLS and balloon data, we do not observe a systematic high MLS bias in these comparisons of the same magnitude (about 15%) that is observed between MLS and HALOE HCl; this argues against most of this bias being caused by MLS-related errors. In terms of future related work, we expect that analyses of the January 2006 balloon campaign from Kiruna, Sweden, will provide a different and interesting view of chlorine partitioning, for comparison to the MLS HCl (and ClO) measurements, under the photochemically perturbed conditions inside the winter Arctic vortex.

[43] Analyses of averaged MLS HCl versus WB-57 (aircraft) in situ HCl from the CIMS measurements during three aircraft campaigns (over Houston in 2004 and 2005, and over Costa Rica in early 2006), coupled with the use of HCl versus O_3 correlation diagrams, help to bring out systematic high biases of ~0.2 ppbv in MLS HCl for the largest pressure (147 hPa) at which the MLS retrievals are performed. MLS and CIMS HCl comparisons at lower

Table 2. Summary of MLS v2.2 HCl Characteristics at Selected Pressure Levels

Pressure, hPa	Resolution, Vertical × Horizontal,[a] km	Precision[b] ppbv	Precision[b] %	Accuracy[c] ppbv	Accuracy[c] %	Comments
≤0.1	–	–	–	–	–	not recommended for scientific use
0.15	6 × 400	1.2	40	0.25	8	
0.2	6 × 350	0.9	30	0.25	8	
0.5	5 × 350	0.7	20	0.15	5	
1	4 × 300	0.5	15	0.15	5	
2	3 × 250	0.4	15	0.15	6	
5	3 × 200	0.3	10	0.2	7	
10	3 × 200	0.2	10	0.2	10	
22	3 × 200	0.2	15	0.1	10	
46	3 × 300	0.2	10 to >40	0.2	10 to >40	% values vary strongly with latitude
68	3 × 350	0.2	15 to >80	0.2	15 to >80	% values vary strongly with latitude
100	3 × 350	0.3	30 to >100	0.15	15 to >100	% values vary strongly with latitude
147	3 × 400	0.4	50 to >100	0.3	50 to >100	may be useful at high latitudes, but high bias at low latitudes (not recommended for scientific use)
>147	–	–	–	–	–	not recommended for scientific use (not retrieved for pressures >147 hPa)

[a]Horizontal resolution is in the along-track direction, and the (along-track) separation between adjacent retrieved profiles is 1.5° great circle angle (∼165 km); cross-track resolution is ∼3 km.
[b]Precision is 1σ estimate for individual profiles.
[c]Systematic uncertainty, 2σ estimate of probable magnitude (see text).

pressures (100 and 68 hPa) agree well, despite the significantly different sampling, resolution, and precision characteristics of these in situ and satellite measurements. The vertical gradients in MLS HCl (not shown here) for latitudes poleward of about 40°N appear to behave better than at low latitudes, as the HCl abundances tend to monotonically decrease with decreasing altitude. The potential usefulness of these higher-latitude MLS HCl data down to 147 hPa needs further investigation, as these data are likely to be of acceptable quality; more information on this issue may be obtained from comparisons with balloon data from the Kiruna (2006 winter) campaign. However, we do not recommend the use of the v2.2 HCl data at 147 hPa for latitudes equatorward of 40° latitude, or for abundances less than 0.5 ppbv. The MLS team will investigate the possibility of obtaining more reliable (average) HCl values at 147 hPa on a global scale, and possibly at larger pressures at high latitudes, for a future data version.

[44] Excellent tracking of temporal changes between MLS and ACE-FTS lower stratospheric HCl has been demonstrated throughout the polar winter seasons, both in the North and in the South, from recent analyses by *Santee et al.* [2008]. Information about stratospheric variations relating to the quasi-biennial oscillation (QBO), as well as annual oscillations, are now emerging from analyses of the Aura MLS data products, including HCl [*Schoeberl et al.*, 2008]. We have shown that the v2.2 MLS data track the v1.51 MLS data well as a function of time, on the basis of available data at the time of writing; this should provide continued critical information about expected stratospheric chlorine decreases [*Froidevaux et al.*, 2006b], as well as constraints on age of air and stratospheric transport issues. We expect that the newly validated v2.2 MLS HCl measurements from Aura will provide many more years of useful global data regarding this key stratospheric chlorine compound.

[45] **Acknowledgments.** This work at the Jet Propulsion Laboratory, California Institute of Technology, was performed under contract with NASA. We are very grateful to the MLS instrument and data/computer operations and development team (at JPL and from Raytheon, Pasadena) for their support through all the phases of the MLS project, in particular D. Flower, G. Lau, J. Holden, R. Lay, M. Loo, G. Melgar, D. Miller, B. Mills, M. Echeverri, E. Greene, A. Hanzel, A. Mousessian, S. Neely, C. Vuu, and P. Zimdars. We greatly appreciate the efforts of B. Bojkov and the Aura Validation Data Center (AVDC) team, whose work facilitated the MLS validation activities. We also acknowledge the work of the satellite instrument and science teams from HALOE, who provided readily available high-quality data that helped us provide timely validation analyses for the MLS retrievals. Thanks to the Aura Project for their support throughout the years (before and after the Aura launch), in particular M. Schoeberl, A. Douglass (also as cochair of the Aura validation working group), E. Hilsenrath, and J. Joiner. We also acknowledge the support from NASA Headquarters, P. DeCola for MLS and Aura, and M. Kurylo and H. Maring, especially, in relation to the Aura validation activities and campaign planning efforts. The aircraft campaigns themselves involved tireless hours of planning from various coordinators, including E. J. Jensen, P. A. Newman, D. W. Fahey, as well as K. Thompson and others involved with campaign flight management and support. We express our thanks to the CIMS and ozone in situ instrument and data analysis teams for their efforts in association with the AVE field experiments and to the Columbia Scientific Balloon Facility for launching the balloon experiments whose data are used in this work. Funding for ACE was provided by the Canadian Space Agency and the Natural Sciences and Engineering Research Council (NSERC) of Canada. The CIMS HCl measurements were supported by the NASA Upper Atmospheric Research Program and the NOAA Atmospheric Chemistry and Climate Program.

References

Anderson, J., J. M. Russell, S. Solomon, and L. E. Deaver (2000), Halogen Occultation Experiment confirmation of stratospheric chlorine decreases in accordance with the Montreal protocol, *J. Geophys. Res.*, *105*, 4483–4490, doi:10.1029/1999JD901075.

Bernath, P. F., et al. (2005), Atmospheric Chemistry Experiment (ACE): Mission overview, *Geophys. Res. Lett.*, *32*, L15S01, doi:10.1029/2005GL022386.

Boone, C. D., et al. (2005), Retrievals for the Atmospheric Chemistry Experiment Fourier-Transform Spectrometer, *Appl. Opt.*, *44*, 7218–7231, doi:10.1364/AO.44.007218.

Chipperfield, M. P. (1999), Multiannual simulations with a three-dimensional chemical transport model, *J. Geophys. Res.*, *104*, 1781–1805, doi:10.1029/98JD02597.

Considine, D. B., M. Natarajan, T. D. Fairlie, G. S. Lingenfelser, R. B. Pierce, L. Froidevaux, and A. Lambert (2008), Noncoincident validation of Aura MLS observations using the Langley Research Center Lagrangian Chemistry and transport model, *J. Geophys. Res.*, doi:10.1029/2007JD008770, in press.

Froidevaux, L., and A. Douglass (Eds.) (2001), Earth Observing System (EOS) Aura science data validation plan, report, version 1.0, NASA Goddard Space Flight Cent., Greenbelt, Md.

Froidevaux, L., J. W. Waters, W. G. Read, P. S. Connell, D. E. Kinnison, and J. M. Russell III (2000), Variations in the free chlorine content of the stratosphere (1991–1997): Anthropogenic, volcanic, and methane influences, *J. Geophys. Res.*, *105*, 4471–4481, doi:10.1029/1999JD901039.

Froidevaux, L., et al. (2006a), Early validation analyses of atmospheric profiles from EOS MLS on the Aura satellite, *IEEE Trans. Geosci. Remote Sens.*, *44*(5), 1106–1121, doi:10.1109/TGRS.2006.864366.

Froidevaux, L., et al. (2006b), Temporal decrease in upper atmospheric chlorine, *Geophys. Res. Lett.*, *33*, L23812, doi:10.1029/2006GL027600.

Froidevaux, L., et al. (2008), Validation of Aura Microwave Limb Sounder stratospheric ozone measurements, *J. Geophys. Res.*, doi:10.1029/2007JD008771, in press.

Jarnot, R. F., V. S. Perun, and M. J. Schwartz (2006), Radiometric and spectral performance and calibration of the GHz bands of EOS MLS, *IEEE Trans. Geosci. Remote Sens.*, *44*, 1131–1143, doi:10.1109/TGRS.2005.863714.

Jiang, Y. B., et al. (2007), Validation of Aura Microwave Limb Sounder ozone by ozonesonde and lidar measurements, *J. Geophys. Res.*, *112*, D24S34, doi:10.1029/2007JD008776.

Johnson, D. G., K. W. Jucks, W. A. Traub, and K. V. Chance (1995), Smithsonian stratospheric far-infrared spectrometer and data reduction system, *J. Geophys. Res.*, *100*, 3091–3106, doi:10.1029/94JD02685.

Lary, D. J., and O. Aulov (2008), Space-based measurements of HCl: Intercomparison and historical context, *J. Geophys. Res.*, *113*, D15S04, doi:10.1029/2007JD008715.

Livesey, N. J. , et al. (2005), Version 1.5 level 2 data quality and description document, *Tech. Rep. JPL D-32381*, Jet Propul. Lab., Pasadena, Calif.

Livesey, N. J., et al. (2006), Retrieval algorithms for the EOS Microwave Limb Sounder (MLS), *IEEE Trans. Geosci. Remote Sens.*, *44*(5), 1144–1155, doi:10.1109/TGRS.2006.872327.

Livesey, N. J., et al. (2008), Validation of Aura Microwave Limb Sounder O_3 and CO observations in the upper troposphere and lower stratosphere, *J. Geophys. Res.*, *113*, D15S02, doi:10.1029/2007JD008805.

Mahieu, E., P. Duchatelet, R. Zander, P. Demoulin, C. Servais, C. P. Rinsland, M. P. Chipperfield, and M. DeMaziere (2004), The evolution of inorganic chlorine above the Jungfraujoch station: An update, paper presented at XX Quadrennial Ozone Symposium, Int. Ozone Comm., Kos, Greece, 1–8 June.

Manney, G. L., et al. (2007), Solar occultation satellite data and derived meteorological products: Sampling issues and comparisons with Aura Microwave Limb Sounder, *J. Geophys. Res.*, *112*, D24S50, doi:10.1029/2007JD008709.

Marcy, T. P., et al. (2004), Quantifying stratospheric ozone in the upper troposphere with in situ measurements of HCl, *Science*, *304*, 261–265, doi:10.1126/science.1093418.

Marcy, T. P., R. S. Gao, M. J. Northway, P. J. Popp, H. Stark, and D. W. Fahey (2005), Using chemical ionization mass spectrometry for detection of HNO_3, HCl, and $ClONO_2$ in the atmosphere, *Int. J. Mass Spectrom.*, *243*, 63–70, doi:10.1016/j.ijms.2004.11.012.

McHugh, M., B. Magill, K. A. Walker, C. D. Boone, P. F. Bernath, and J. M. Russell III (2005), Comparison of atmospheric retrievals from ACE and HALOE, *Geophys. Res. Lett.*, *32*, L15S10, doi:10.1029/2005GL022403.

Nassar, R., et al. (2006), A global inventory of stratospheric chlorine in 2004, *J. Geophys. Res.*, *111*, D22312, doi:10.1029/2006JD007073.

Proffitt, M. H., and R. L. McLaughlin (1983), Fast-response dual-beam UV-absorption ozone photometer suitable for use on stratospheric balloons, *Rev. Sci. Instrum.*, *54*, 1719–1728, doi:10.1063/1.1137316.

Read, W. G., Z. Shippony, M. J. Schwartz, N. J. Livesey, and W. V. Snyder (2006), The clear-sky unpolarized forward model for the EOS Microwave Limb Sounder (MLS), *IEEE Trans. Geosci. Remote Sens.*, *44*(5), 1367–1379, doi:10.1109/TGRS.2006.873233.

Read, W. G., et al. (2007), Aura Microwave Limb Sounder upper tropospheric and lower stratospheric H_2O and relative humidity with respect to ice validation, *J. Geophys. Res.*, *112*, D24S35, doi:10.1029/2007JD008752.

Rinsland, C. P., et al. (2003), Long-term trends in inorganic chlorine from ground based infrared solar spectra: Past increases and evidence for stabilization, *J. Geophys. Res.*, *108*(D8), 4252, doi:10.1029/2002JD003001.

Rinsland, C. P., et al. (2005), Trends of HF, HCl, CCl_2F_2, CCl_3F, $CHClF_2$ (HCFC-22), and SF6 in the lower stratosphere from Atmospheric Chemistry Experiment (ACE) and Atmospheric Trace Molecule Spectroscopy (ATMOS) measurements near 30 N latitude, *Geophys. Res. Lett.*, *32*, L16S03, doi:10.1029/2005GL022415.

Rodgers, C. D. (1976), Retrieval of atmospheric temperature and composition from remote measurements of thermal radiation, *Rev. Geophys.*, *14*, 609–624, doi:10.1029/RG014i004p00609.

Russell, J., et al. (1993), The Halogen Occultation Experiment, *J. Geophys. Res.*, *98*, 10,777–10,798, doi:10.1029/93JD00799.

Russell, J. M., III, et al. (1996), Validation of hydrogen chloride measurements made by the Halogen Occultation Experiment from the UARS platform, *J. Geophys. Res.*, *101*(D6), 10,151–10,162.

Santee, M. L., G. L. Manney, J. W. Waters, and N. J. Livesey (2003), Variations and climatology of ClO in the polar lower stratosphere from UARS Microwave Limb Sounder measurements, *J. Geophys. Res.*, *108*(D15), 4454, doi:10.1029/2002JD003335.

Santee, M. L., et al. (2008), Validation of Aura Microwave Limb Sounder ClO measurements, *J. Geophys. Res.*, doi:10.1029/2007JD008762, in press.

Schneider, M., T. Blumenstock, M. P. Chipperfield, F. Hase, W. Kouker, T. Reddmann, R. Ruhnke, E. Cuevas, and H. Fischer (2005), Subtropical trace gas profiles determined by ground-based FTIR spectroscopy at Izana (28°N, 16°W): Five-year record, error analysis, and comparison with 3-D CTMs, *Atmos. Chem. Phys.*, *5*, 153–167.

Schoeberl, M. R., et al. (2006), Overview of the EOS Aura mission, experiment, *IEEE Trans. Geosci. Remote Sens.*, *44*(5), 1066–1074, doi:10.1109/TGRS.2005.861950.

Schoeberl, M. R., et al. (2008), QBO and annual cycle variations in tropical lower stratosphere trace gases from HALOE and Aura MLS observations, *J. Geophys. Res.*, *113*, D05301, doi:10.1029/2007JD008678.

Schwartz, M. J., W. G. Read, and W. V. Snyder (2006), EOS MLS forward model polarized radiative transfer for Zeeman-split oxygen lines, *IEEE Trans. Geosci. Remote Sens.*, *44*, 1182–1191, doi:10.1109/TGRS.2005.862267.

Schwartz, M. J., et al. (2008), Validation of Aura Microwave Limb Sounder temperature and geopotential height measurements, *J. Geophys. Res.*, doi:10.1029/2007JD008783, in press.

Solomon, P., J. Barrett, T. Mooney, B. Connor, A. Parrish, and D. E. Siskind (2006), Rise and decline of active chlorine in the stratosphere, *Geophys. Res. Lett.*, *33*, L18807, doi:10.1029/2006GL027029.

Toon, G. C. (1991), The JPL MkIV interferometer, *Opt. Photon. News*, *2*, 19–21.

Waters, J. W., et al. (1996), Validation of UARS Microwave Limb Sounder ClO measurements, *J. Geophys. Res.*, *101*, 10,091–10,127, doi:10.1029/95JD03351.

Waters, J. W., et al. (2006), The Earth Observing System Microwave Limb Sounder (EOS MLS) on the Aura satellite, Experiment, *IEEE Trans. Geosci. Remote Sens.*, *44*(5), 1075–1092, doi:10.1109/TGRS.2006.873771.

Webster, C. R., R. D. May, D. W. Toohey, L. M. Avallone, J. F. Anderson, and S. Solomon (1993), In situ measurements of the ClO/HCl ratio: Heterogeneous processing on sulfate aerosols and polar stratospheric clouds, *Geophys. Res. Lett.*, *20*, 2523–2526, doi:10.1029/93GL01963.

Webster, C. R., et al. (1994), Hydrochloric acid and the chlorine budget of the lower stratosphere, *Geophys. Res. Lett.*, *21*, 2575–2578, doi:10.1029/94GL02806.

Wu, D. L., et al. (2008), Validation of the Aura MLS cloud ice water content measurements, *J. Geophys. Res.*, doi:10.1029/2007JD008931, in press.

Zander, R., et al. (1996), The 1994 northern and mid-latitude budget of stratospheric chlorine derived from ATMOS/ATLAS 3 observations, *Geophys. Res. Lett.*, *23*, 2357–2360, doi:10.1029/96GL01792.

P. F. Bernath, Department of Chemistry, University of York, York YO10 5DD, UK.

C. D. Boone and K. A. Walker, Department of Chemistry, University of Waterloo, Waterloo, ON, Canada N2L 3G1.

L. E. Christensen, R. E. Cofield, D. T. Cuddy, W. H. Daffer, B. J. Drouin, L. Froidevaux, R. A. Fuller, R. F. Jarnot, Y. B. Jiang, B. W. Knosp, A. Lambert, N. J. Livesey, G. L. Manney, V. S. Perun, W. G. Read, M. J. Schwartz, W. V. Snyder, R. A. Stachnik, P. C. Stek, R. P. Thurstans, G. C. Toon, P. A. Wagner, J. W. Waters, and C. R. Webster, Jet Propulsion Laboratory, California Institute of Technology, Pasadena, CA 91109, USA. (lucien.froidevaux@jpl.nasa.gov)

D. W. Fahey, R. S. Gao, and P. J. Popp, Earth System Research Laboratory, NOAA, Boulder, CO 80305, USA.

R. S. Harwood and H. C. Pumphrey, School of GeoSciences, University of Edinburgh, Edinburgh EH9 3JW, UK.

K. W. Jucks, Harvard-Smithsonian Center for Astrophysics, Cambridge, MA 02138, USA.

T. P. Marcy, 730 N. 23rd Street #300, Milwaukee, WI 53233, USA.